Russian Geology and Geophysics
Vol. 47, No. 3, pp. 315-341, 2006

Geologiya i Geofizika
UDC 553.441(571.53)

THE GIANT SUKHOI LOG GOLD DEPOSIT, SIBERIA

B.L. Wood[1] and N.P. Popov*

StarTechnology Systems N.L., Moscow, Russia,
PO Box 6325, University of NSW, Sydney, NSW 1466, Australia
** Lenzoloto Open Joint Stock Company,*
Bodaibo, Russia

The Sukhoi Log gold deposit is centrally located in the Lena goldfield region, approximately 850 km NE from the city of Irkutsk, and is hosted in Upper Proterozoic marine sandstone, carbonaceous slate and phyllite, metamorphosed to low greenschist facies in an outlying part of the major Akitkan Foldbelt. The disseminated pyritic tabular orebody has no outcrop, is defined solely by assay grades and is located in the axial zone of a large, near-isoclinal, reclining anticline. Highest ore grades occur in pyritic black shale beds, especially where they cross the axial zone and include two elongate higher grade (4–9 ppm gold) cylindrical zones, termed ore pillars, along the gently plunging anticlinal crest. The anticline is exposed E-W over a length of 3 km and plunges at approximately 10° degrees NW. The axial plane and orebody dip 15° N, and the latter is open to depth beyond 400 m. Three phases of syn- and post-metamorphic mesoscopic folding developed characteristic structures. The first two (F_1 and F_2) are congruent with the anticline and localized quartz-pyrite-gold veinlet mineralization in F_1 axial plane cleavages (S_1), in narrow, spaced axial zones of small non-penetrative folds (F_2), in irregular disseminated zones in shale, and in small irregular clusters (stringers) of quartz-carbonate veins. A third phase generated scattered kink-fold bands (F_3) and irregular crumpled zones without mineralization. A later episode of transgressive mesothermal quartz-vein mineralization developed many low-grade auriferous veins that have been the main sources of the extensive alluvial gold deposits.

The mineralization assemblage is consistently quartz-pyrite-gold carbonate with minor base and platinum group metals. Pyrite is widely distributed in black shale throughout the deposit, at between 2 and 5 percent, and in lesser amounts in a disseminated envelope around the orebody. In the outer parts of the orebody and in the enclosing mineralization envelope it contains gold of higher fineness (900–920), whereas clustered and veinlet pyrite is more common in the interior productive zone, with gold of lower fineness (840–880). The deposit was intensively explored from October 1971 to December 1977. The orebody at a cutoff grade of 1 ppm gold, is an elongate irregular planoconvex sheet up to 140 m thick, dipping NNE at 15° to 30°, with a length of 2.2 km, a down dip width of more than 500 m, and is probably open to depth. It contains 384 million tonnes with an average grade of 2.5 to 2.7 grams per tonne. Additional resources include 165 million tonnes at 2.0 to 2.3 ppm in a low grade, possible pit extension, and 205 million tonnes at 0.8 ppm in the mineralization envelope.

Sequences of pyrite-gold paragenesis, of textural and structural changes, and limited isotope data indicate that four distinct stages of mineralization occurred during MOR subduction and Riphean closure of the major Proterozoic Akitkan Foldbelt.

Disseminated, pyritic, synmetamorphic, greenschist, gold-PGM, Lena, Patom, Baikal, Riphean, Neoproterozoic, Late Precambrian, ridge-subduction, Akitkan, Olokit

1 Corresponding author: brycelwood@hotmail.com

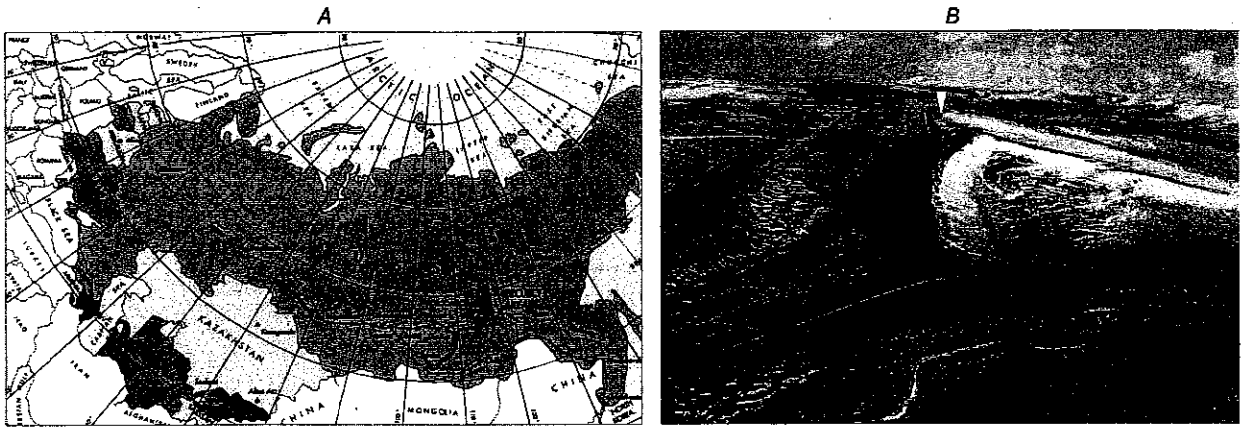

Fig. 1. *A* **— Location map.** *B* **— Sukhoi Log hill, view west. The orebody is an extensive flat sheet that underlies the ridge (V) behind the higher summit in centre and dips north to the right under the snowfield. Two cleared lines on left are for a road and powerline to a future plant site; the valley in left centre with alluvial workings is named Sukhoi Log, translated as Dry Gulch.**

INTRODUCTION

The Sukhoi Log gold deposit in Siberia (Fig. 1, *A*) was discovered in 1961 and intensively explored in the 1970s. Many detailed internal reports were written and a few papers published in Russian, but little is known of the deposit outside of Russia because of former official secrecy restrictions. The following account is based on much detailed information in Departmental and Institute archives that were available to the authors during a lengthy feasibility study from 1993 to 1996, but many are not yet accessible for general reference outside Russia. In addition to the following geological account, the origin of the disseminated sediment-hosted mineralization is explained in some detail as the result of the collision of a MOR spreading zone with a Late Proterozoic subduction zone.

HISTORY OF DISCOVERY

The exploration for and discovery of the Sukhoi Log gold deposit was the culmination of many years of study and development of the Lena goldfields by several generations of geologists and miners. The deposit is entirely "blind", that is, it has no surface outcrop, and it was discovered not by prospectors using traditional methods, but by geologists using new concepts of ore deposition, state-of-the-art methods of geochemical prospecting, and ultimately diamond drilling.

The history of goldfields in the Lena region dates back to 1846 when the first alluvial gold deposits were discovered in the valley of the Khomolkho River 30 km NE of Sukhoi Log. In the 1860s rich alluvial gold deposits were found in many widespread localities, including the small valleys on the north and south sides of Sukhoi Log hill, named Radostny, Zorinski and Sukhoi Log (or Dry Gulch) (Fig. 1, *B*). More than 30 t of gold was extracted from these three alluvial deposits between 1863 and 1900. The crest of the watershed there exposed many large gold-bearing quartz vein outcrops on which the mine Sergiev was started on top of the hill in 1886, and the mine Utesisty in 1894. The main targets for primary gold during 1899–1904 were these and other quartz veins, from which about 1 t of gold was mined during prospecting, but gold recovery proved difficult and the work was often not profitable.

In the 1960s geologist V.A. Buryak proposed on the basis of known geochemically anomalous gold in Sukhoi Log rock samples that sulfide-gold ore may be present and that this should be a major exploration objective [1, 2]. The first drillholes that followed in the spring and summer of 1961 revealed gold-bearing sulfide mineralization at depth, and verified Buryak's proposition. Further drilling and feasibility studies were undertaken up to 1971 by Irgiredmet in Irkutsk, and very intensive exploration started in the autumn of 1971 and was completed at the end of 1977. The work included 209.6 km of diamond core drilling in 846 drillholes, 11.7 km of underground drives (Nos. 1 and 2), 61 raises, 1,546 m of which were in ore, 110.3 km of trenches, 13,000 channel samples, three

bulk samples of 150 t, 800 t, and 980 t, many tens of thousands of assays for gold, and many analyses for other purposes.. The data are preserved as voluminous archives in Russian at Bodaibo, Moscow, and various Institutes elsewhere, and provide a very detailed database of the deposit.

In addition to the Sukhoi Log deposit, several lesser gold deposits of the same type were discovered in the region with considerably smaller reserves, but nevertheless would collectively support major mining and production. These include Verninsky, Vysochaishy, Nevsky, and two small, physically separate lensoid orebodies in the flanks and lower levels of the Sukhoi Log deposit, named Central Radostny and Zapadny Radostny.

The two major underground drives (Nos. 1 and 2) of the 1970s program were re-opened in 1995, and provided direct access to and observation of a large part of the interior of the orebody for purposes of the feasibility study that was conducted in 1993–96 by Star Mining Corporation, Sydney, Australia.

LOCATION, TERRAIN AND ACCESS

The Lenzoloto project area lies between 57 and 60 degrees North latitude, approximately 900 km south of the Arctic Circle (Fig. 1, *A*) and is 105,000 km^2 in area (Fig. 2). The climate is strongly continental with average temperatures of –21 °C in January and +18 °C in July and with a maximum-minimum range of +30 °C to –50 °C. The winter months from October to May are generally dry and windless with heavy snow and ice formation, and all waterways are frozen. The summers are warm and mostly dry.

The region comprises a broad, subcircular topographic dome approximately 350 km in diameter, termed the Patom Highland, that rises to altitudes of 1650 m in the centre and to more than 1800 m in the SE. It is partly encircled by the Vitim and Lena Rivers, and dissected by several tributary river systems that exhibit well-defined concentric and radially divergent trends (Fig. 2). The terrain is one of extensive high rounded ridges with some steep slopes along scarps of sedimentary rocks (Fig. 1, *B*). The major high level landforms developed under several episodes of Pleistocene ice-sheet erosion, a late phase of trunk valley glaciation, lengthy periods of periglacial erosion, and several phases of interglacial warm climate chemical erosion. The deep alluvial and colluvial deposits in most channels and river valleys result from long periods of gentle drainage and glacial erosion.

Siberian forest (taiga) consisting of birch, maple, pine, cedar, spruce and larch covers mountain slopes and some valleys up to about 1,200 m above sea level. Upland areas and broad crests carry a sparse cover of subarctic shrubs, or more commonly consist of extensive rockfields occasionally with periglacial patterned ground and rock streams.

Regular airline services operate between the city of Irkutsk and the Lena goldfields township of Bodaibo, (pop. ~40,000), from which road access is available to all outlying villages and operations.

REGIONAL GEOLOGY

The regional geological setting of Sukhoi Log and the Lena goldfield is that of a complex folded sedimentary sequence at the exposed northeast end of the Akitkan Foldbelt and the included Olokit Zone, parts of both of which extend into the western side of the goldfield area as shown in Fig. 3. The 250 km southwesterly extension of the Olokit Zone, and the 800 km of the Akitkan Foldbelt are exposed in the mountainous Primorsky Range along the western shore of Lake Baikal. Geophysical evidence suggests that the total length of the Foldbelt including that which is concealed to the northeast beneath Phanerozoic platform cover, may be more than 1,500 km, and its width is between 50 and 250 km (Fig. 3). It is thus a major Proterozoic orogenic belt within the Siberian craton, between the Aldan Shield to the east and the Magan Province to the west. Thick formational units in the Olokit Zone of the Akitkan Foldbelt are exposed along the western side of the Patom Highlands between the Abchad and Vilyui Faults in the Mama township district (see Fig. 3). In contrast, a much thinner condensed Patom sequence (see Figs. 3 and 4) overlies Archean high-grade gneiss and Chara metasediments of the Aldan Shield on the southeastern side of the Highlands.

Stratigraphy. The Patom Highland exposes strongly folded rocks mainly of Proterozoic age, and is surrounded on three sides by flat-lying Paleozoic and younger cover of the Siberian Platform (Fig. 3). The stratigraphic sequences of the Upper Proterozoic are well developed and are represented by deposits of marine shelf, slope and euxinic basinal facies [3].

In summary, the Precambrian sequence of the region (Figs. 3 and 4) consists of the following:

1. Archean high-grade rocks (Chara units) of the Aldan Shield, exposed locally in the SE; gneiss, migmatite, slate, quartzite.

2. A minor Early Proterozoic sequence unconformable on the Aldan, of slates and quartzites (Nerukan

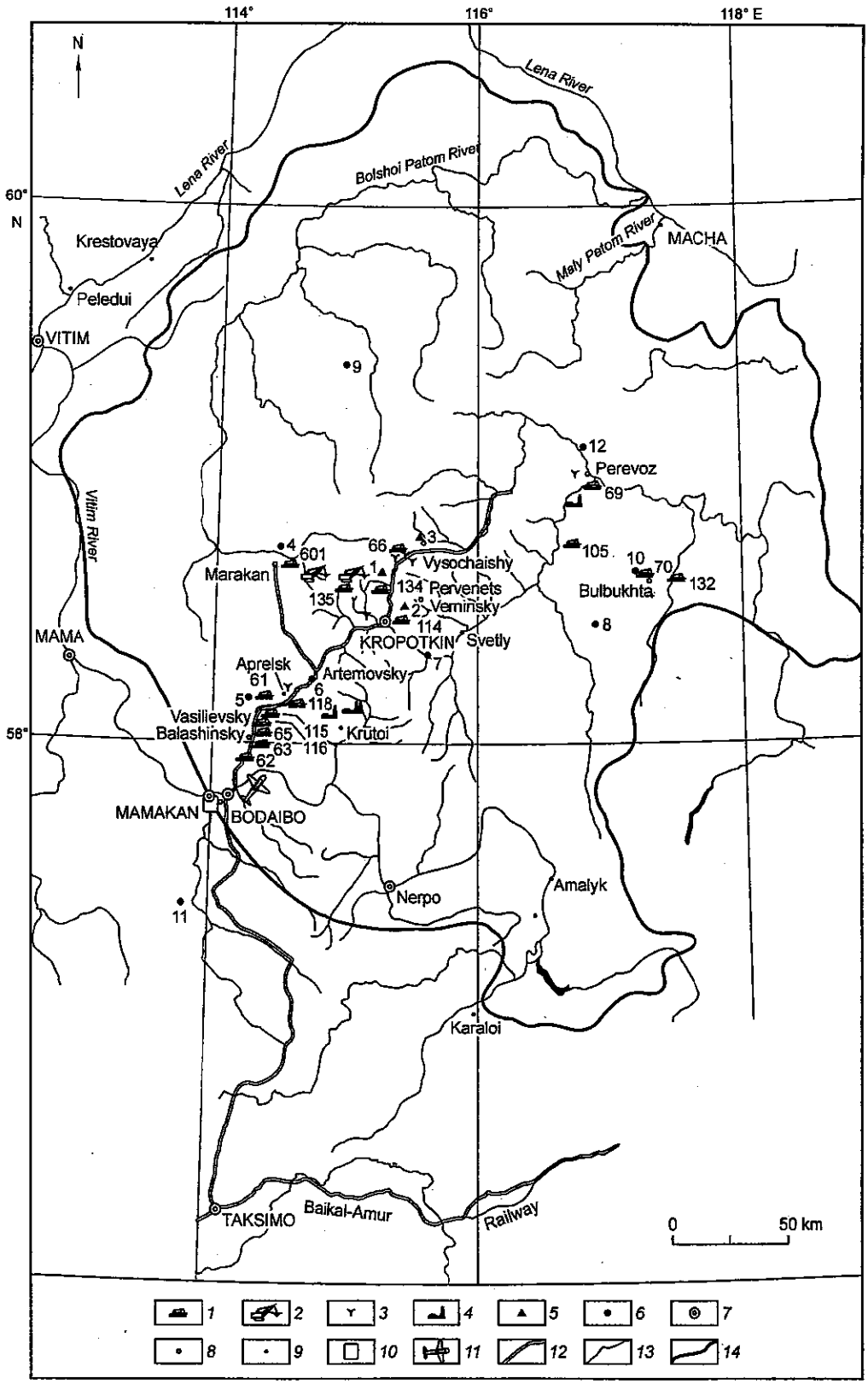

Fig. 2. Area of operations. *1* **— dredging,** *2* **— mechanical excavating,** *3* **— panning,** *4* **— mines. Primary deposits: 1 — Sukhoi Log, 2 — Pervenets-Vernensky, 3 — Vysochaishy. Main alluvial deposits: 4 — Shusman, 5 — Vasilievsky, 6 — Artemovsky, 7 — Ust'-Dzhegdakar, 8 — Khodokan, 9 — Chertovo Koryto, 10 — Bulbukhta, 11 — Mama-Vitim, 12 — Dalnyaya Taiga.** *7* **— district centers,** *8* **— mining districts and prospect bases,** *9* **— villages,** *10* **— hydroelectrical plant,** *11* **— main airport,** *12* **— dirt roads,** *13* **— rivers,** *14* **— administrative boundary.**

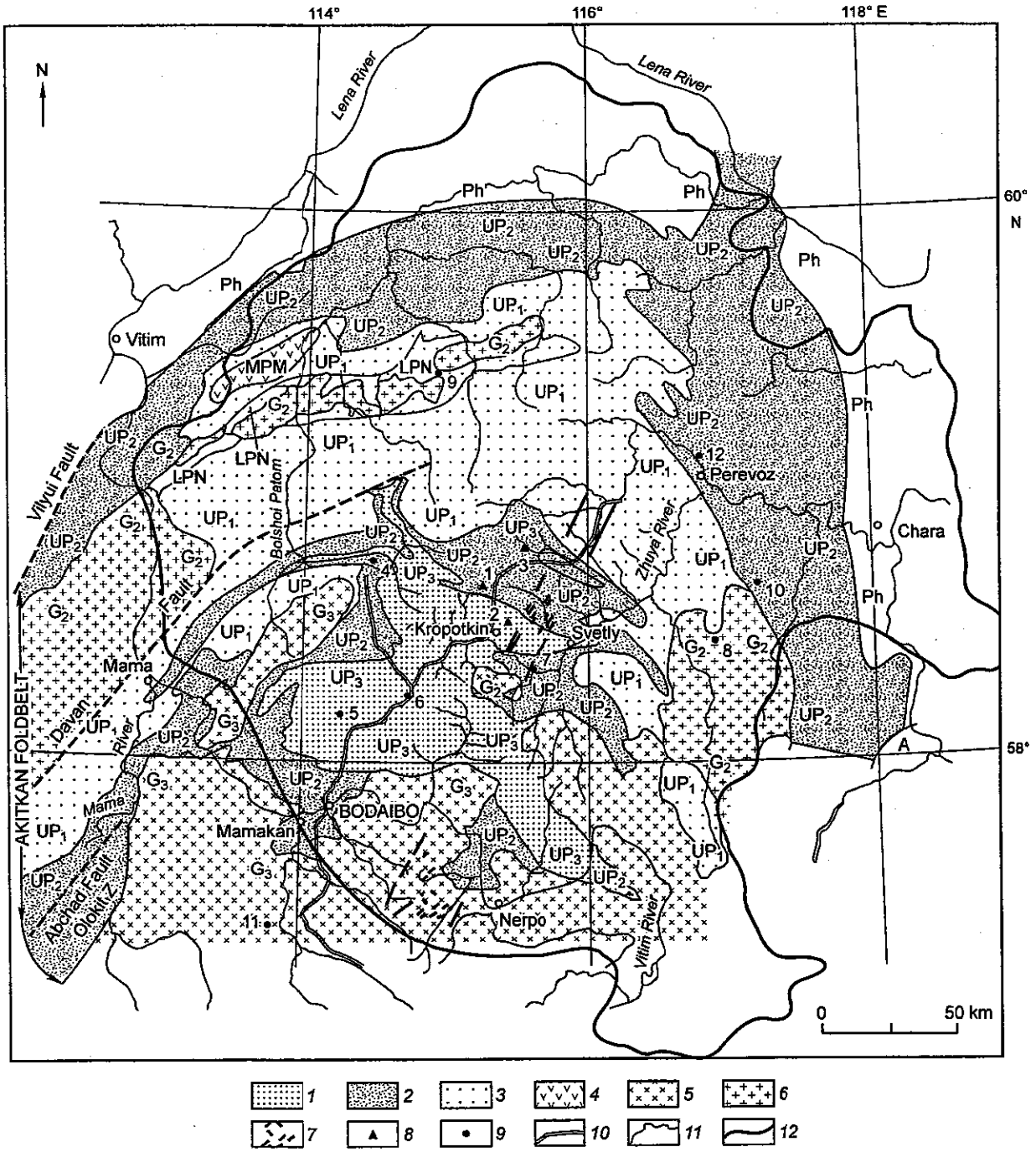

Fig. 3. Geological map of the Lena-Bodaibo goldfields area (modified in part from [6, 12, 27]. Ph — Phanerozoic (platform cover); UP — Upper Proterozoic (Patom Group): *1* — fine carbonaceous clastics and limestones, Upper Patom (Bodaibo units), UP_3; *2* — marble, carbonaceous sandstone and slate, Middle Patom (Kadalik units), UP_2; *3* — conglomerate, quartzite, slate, Lower Patom (Balanganakh units), UP_1; *4* — MP — Mesoproterozoic, MPM — Medvezh'ya Formation — volcanic and sedimentary rocks; LP — Lower Proterozoic, LPN — Nerukan unit — quartzite slate; A — Archean (Chara units) — high-grade gneiss, quartzite, slate. Intrusive rocks: *5* — Paleozoic granites, pyroxene granites, granodiorite, G_3 — Upper Proterozoic to Eocambrian. *6* — undifferentiated Lower and Middle Proterozoic granite, gneiss, diabase, migmatite, local volcanic rocks, G_2. *7* — regional dike belt, with basic and lamprophyric dikes shown. *8* — primary disseminated gold deposits: 1 — Sukhoi Log, 2 — Pervenets-Vernensky, 3 — Vysochaishy. *9* — primary vein gold deposits: 4 — Shusman, 5 — Vasilievsky, 6 — Artemevsky, 7 — Ust'-Dzhegdakar, 8 — Khodokan, 9 — Chertovo Koryto. 10 — Bulbukhta, 11 — Mama-Vitim, 12 — Dalnyaya Taiga. *10* — roads; *11* — rivers; *12* — administrative boundary.

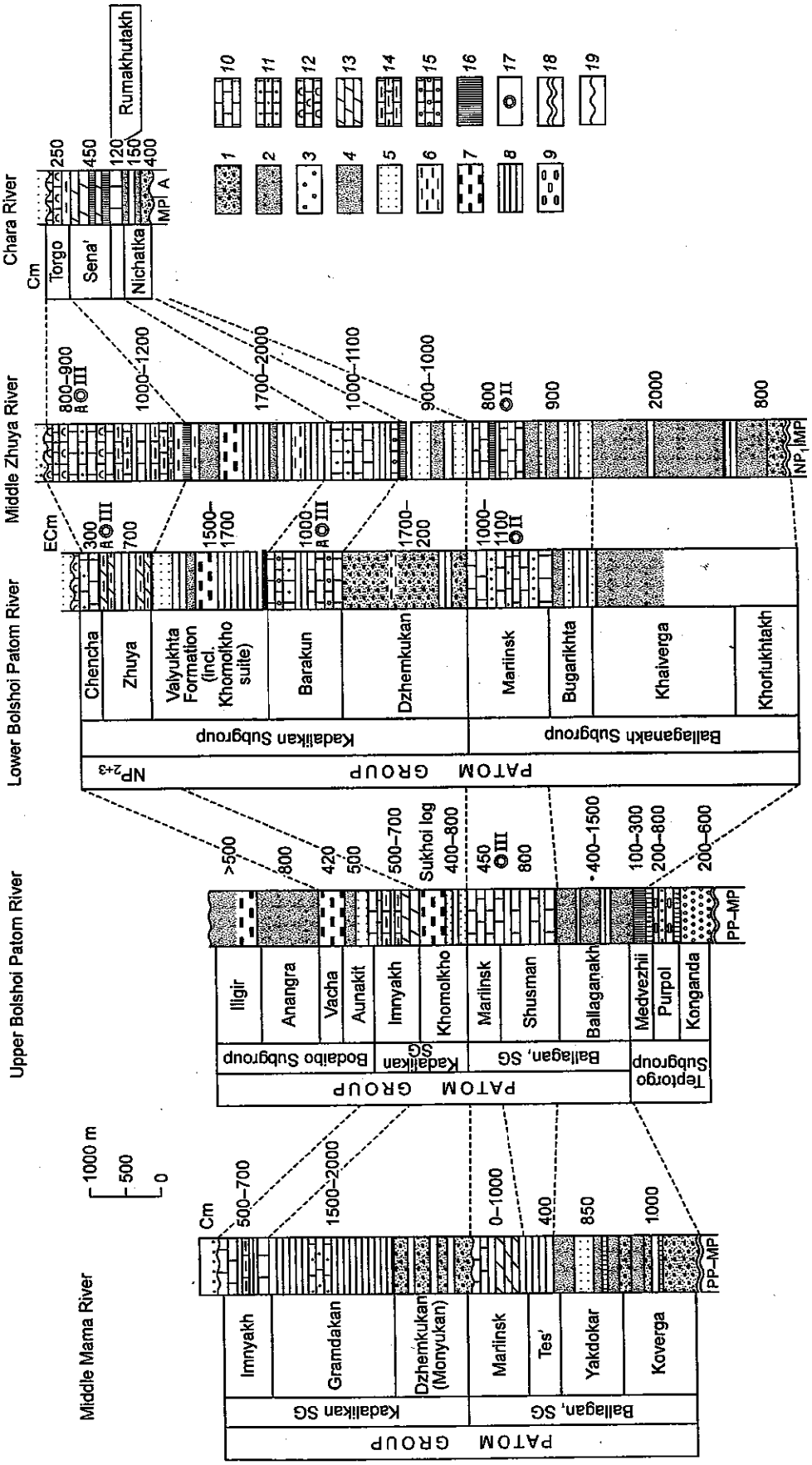

Fig. 4. Correlation of the Neoproterozoic sequences in different zones of the Lena goldfields area [6]. *1* — conglomerate, *2* — gritstone (among sandstone), *3* — arkose, *4* — oligomictic and polymictic sandstone, *5* — quartzite-sandstone (quartzite), *6* — siltstone, *7* — carbonaceous slate and quartzite, *8* — shale (slate, phyllite) partially siltstone, *9* — chloritoid slate, *10* — limestone, *11* — oncolitic limestone, *12* — stromatolitic limestone and dolomite, *13* — dolomite, *14* — marl, calcareous slate, *15* — carbonate breccia and conglomerate, *16* — chlorite slate, basic volcanics, *17* — microfossils, *18* — angular unconformity, *19* — disconformity. A — Archean, PP — Paleoproterozoic, MP — Mesoproterozoic, NP_1 — Lower Proterozoic, EP — Epiproterozoic, ECm — Eocambrian, Cm — Cambrian.

Formation), and a few Lower and Middle Proterozoic spilites, keratophyres, chlorite-slates and basic volcanics (Medvezh'ya Formation) in the western Highlands.

3. The Upper Proterozoic Patom Group, is divided into three main subgroups.

— the lower Ballaganakh Subgroup, with an important component of conglomerate and gritstone;

— the middle Kadalikan Subgroup, dominated by carbonate rocks containing algal remains; this unit hosts the main quartz vein gold deposits of the region and the disseminated pyrite-gold deposit of Sukhoi Log in carbonaceous shales;

— the upper Bodaibo Subgroup, dominated by fine clastic, calcareous and dark carbonaceous rocks which also contain gold deposits of disseminated pyritic type, alternating with rhyolitic molasse-type conglomerates.

4. Numerous intrusive complexes include many varieties of granite, and also a regional NE-SW trending basic dyke belt [3] that lies 20 km east of Sukhoi Log, Vysochaishy and Pervenets-Verninsky (Fig. 3), in which lamprophyre has been dated by the Sm-Nd method at 313±59 Ma [4]. Some of the granites are Early and Middle Proterozoic (Baikalian), others are Paleozoic and are dated at 354 Ma to 322 Ma (Hercynian) [5]. The nearest granite to Sukhoi Log is the small Konstantinovsky stock, 6 km to the SW, which is dated at 290±20 Ma [5].

In the Patom Highland the Bodaibo Subgroup is Epiproterozoic [6], and lies without any apparent unconformity on the Neoproterozoic Kadalikan Subgroup (Fig. 4). The Kadalikan Subgroup increases considerably in thickness northward from the Bodaibo area to the lower Bolshoi Patom River, and in the Sukhoi Log-Kropotkin area includes a sequence of sandstone, carbonaceous shale and phyllite, named the Khomolkho Formation as a local unit of the 1500 m thick Valyukhta Formation (Fig. 4). This unit hosts the pyritic gold mineralization at Sukhoi Log and Vysochaishy.

The uppermost formation of the Kadalikan, the Imnyakh (500–700 m), consists of calcareous slate, siltstone, quartz and mica-quartz sandstone and lesser bands of limestone. The overlying Aunakit Formation (200–1200 m) of the Bodaibo Subgroup consists of polymict sandstone, sericite-quartz shale, and carbonaceous shale which hosts the sulfide-gold mineralization of the Pervenets-Verninsky deposits. Above the Aunakit lie three formations of fine to coarse clastics which aggregate up to 3700 m in thickness.

Structure. The Patom Highland has a distinctive regional structural pattern marked by folds in the Upper Proterozoic metasedimentary units, the axes of which vary systematically in trend from NE in the west to SE in the east. In plan view this forms a semi-circular arrangement with the Marakan-Tungus Trough to the north and the Bodaibo Synclinorium to the south, in the latter of which are the main vein-gold orebodies. Sukhoi Log lies in the anticlinorium between them.

The Patom Group rocks were strongly folded in a major deformation phase accompanied by low-grade regional greenschist facies metamorphism which to the south is locally overprinted by metamorphic aureoles of the Paleozoic granites. The fold traces are convex to the north, towards the Siberian Platform (Fig. 3). In the northern near-platform margin of the Patom Highland, the sediments display great thickness, gentle folding with slight vergence toward the platform and a very low grade of greenschist metamorphism. Fold zones occur farther south in the Bodaibo Synclinorium in which the thickness of the strata is greatly reduced and the rocks are intensely folded and metamorphosed at lower to middle grades of the greenschist facies. The folds are assymmetrical, reclining, near-isoclinal, with vergence "facing" southward to the Mama-Vitim zone. Within the latter zone, the two lower subgroups acquire a great thickness again, display frequent rhythmic alternations of Bouma flyschoid type and extend out of the Lena region as a part of the major Akitkan Foldbelt that extends south to Lake Baikal (Fig. 3). At regional scale, the sequence of deformational events appears to be simple, with first-phase penetrative flexural-slip folding (F_1), generating large first-, second-, and third-order folds, axial plane foliation, schistosity and cleavage. A second phase of lesser deformation is also widespread but is usually evident as locally separate zones of small flexural folds (F_2) that rotate the earlier F_1 foliation structures. F_2 axial planes are usually subvertical, and axial structures are commonly very irregular and nonpenetrative. Both the F_1 and F_2 generations are evident in the Sukhoi Log deposit and have exerted significant local structural control over the mineralization.

A third phase of deformation developed a range of nonpenetrative structures (F_3) such as kink-folds, fold bands, and fault-fold combinations. This phase probably involved several unrelated local episodes, at least one of which included the emplacement of the widespread but subeconomic quartz vein-gold deposits of the Lena goldfields, including those in the Sukhoi Log area (Fig. 5, *A*).

GEOLOGY OF THE DEPOSIT

The following account of the Sukhoi Log geology is based on references cited, on earlier extensive file reports co-authored by N.P. Popov, and on personal observations of the authors.

Earliest reports include an unpublished geological account and map at 1:10,000 by Buryak and Kochetkov

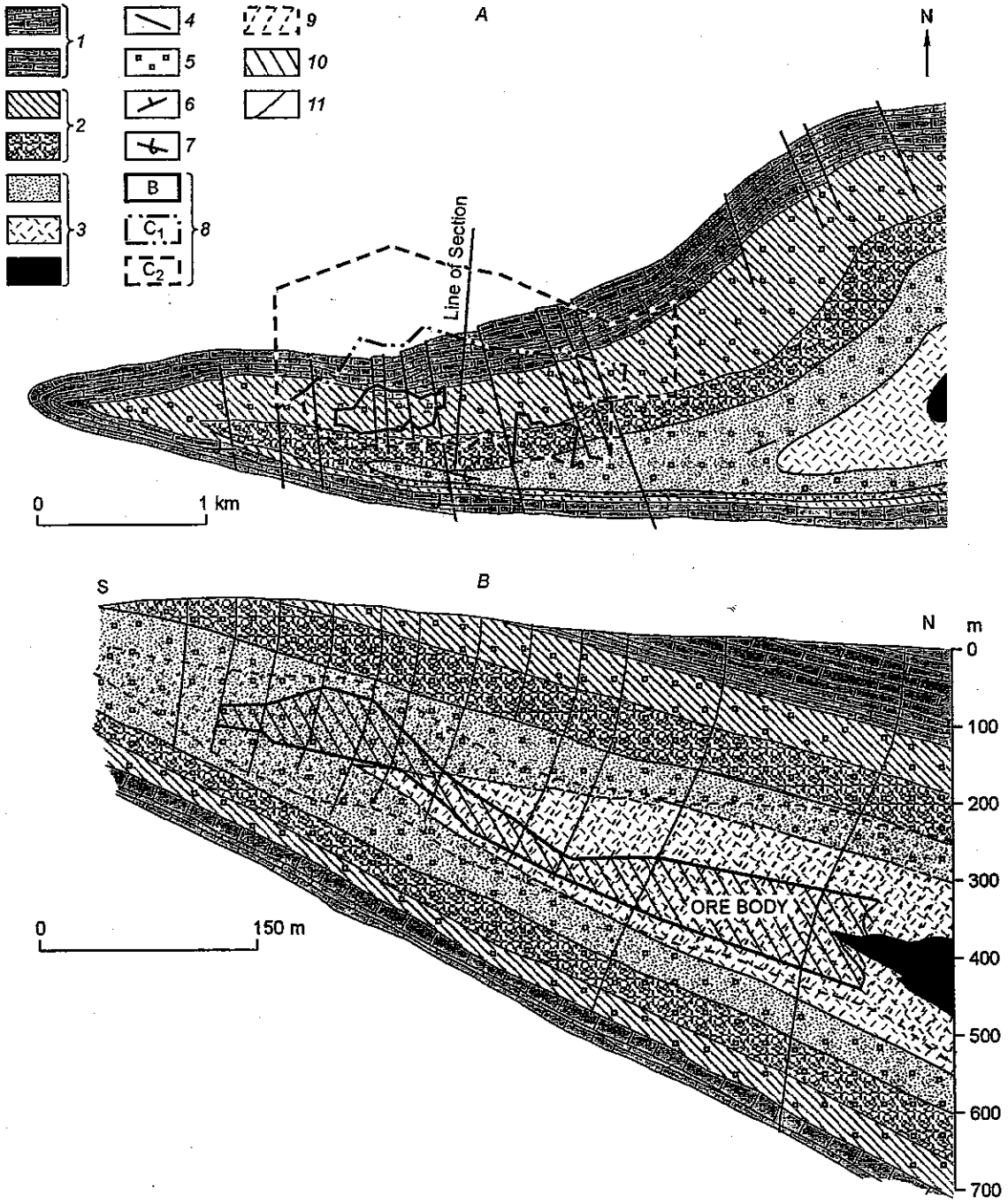

Fig. 5. Schematic plan (*A*) and cross section (*B*), Sukhoi Log; [9], with ore blocks added. *1* — calcareous carbonaceous siltstone and slate; *2* — carbonaceous siltstone, phyllite; *3* — carbonaceous phyllite, slate, siltstone; *4* — faults; *5* — disseminated pyrite; *6* — normal facing bedding; *7* — overturned bedding; *8* — ore blocks defined by drilling and underground development; *9* — mineralization zone; *10* — zone of economic ore; *11* — drill hole.

(1959), and detailed published reports in 1964 [7], and in 1969 [8], on ores and rocks of Sukhoi Log. A brief account and map of the geology and the vein gold deposits of Sukhoi Log was published in 1971 [3] as part of a wider study of the Lena gold-bearing region. A generalized description of the sulfide-gold mineralization, together with a schematic map and section, was published in 1974 [9], and this indicated for the first time the unique

qualities of the deposit. A more detailed account in English was presented by Buryak in 1986 [10], and provides the basis for much of the following. A further report in 1987 discussed the origin of the gold mineralization [11].

Stratigraphy. The stratigraphic sequence of the host rocks of the deposit area consists of two conformable suites of upper Proterozoic age named Khomolkho [hm] and Imnyakh [im]. The Khomolkho Formation is subdivided lithologically into three Subformations, the Lower (hm_1) — carbonaceous shale and siltstone with interlayers of carbonaceous limestone (100–150 m); the Middle (hm_2) grey limestone with interlayers of siltstone and carbonaceous shale (110–200 m); the Upper (hm_3) — carbonaceous shale, phyllite and siltstone (150–180 m).

The overlying Imnyakh Formation is subdivided lithologically in two Subformations: the Lower (im_1) — mainly calcareous sandstone, shale and siltstone, less commonly limestone; and the Upper (im_2) — mainly limestone with interlayers of shale and dolomite.

The ore-bearing zone occurs in the sediments of the Upper Khomolkho Subformation (hm_3) within the hinge zone and limbs of the Sukhoi Log Anticline (see Fig. 5).

Further detailed stratigraphic subdivision of the hm_3 ore-hosting sequence of the Upper Subformation is based on lithology (type and rhythm of lamination, physical properties, cleavage). Five units have been identified in the sequence based on these criteria and are illustrated in detail by Buryak et al. [10].

Intrusive rocks. The small granitoid Konstantinovsky stock is located 6 km to the SW of Sukhoi Log and is a member of the Konkuder-Mamakan complex. It appears at the surface as two adjacent outcrop areas of 0.5 km^2, within a small negative gravity anomaly. Geophysical data indicate that the body has a steep southern contact and a gently sloping northeastern one toward Sukhoi Log. The rock is a biotite porphyrite in the centre, is fine-grained in the contact zone, and is Permian, dated at 290±20 Ma [12]. A 100–250 m wide contact metamorphic aureole surrounds the outcrop, with greater width to the north than the south. Several latitudinal dikes of granite porphyry and quartz porphyry are located nearby.

Other more distant intrusives include large Paleozoic granite domes to the south, ages of which are Carboniferous and range from 354±12 Ma to 330±10 Ma [4]. A NE trending zone of basic and lamprophyric dikes have been dated at 313±59 Ma (also Carboniferous) by the Sm-Nd method; they are cut by late stage 290±20 Ma Permian granite porphyry dikes [4]. All these intrusives represent a major cycle of Hercynian magmatic activity following long after the convergence and suturing of the Akitkan Foldbelt. However there is no evidence to indicate that there were any significant effects on the Sukhoi Log or lesser disseminated gold deposits such as Vysochaishy.

Host rock details. The host rocks of the gold mineralization consist of a monotonous sequence of Khomolkho Formation thin-bedded black shale and siltstone that are considered to have been deposited in one or more restricted anoxic basins. Bedding is evident, at scales of a few centimetres, by alternations of grey siltstone and black shale, and at finer scale by less evident thin layers of fine dark silt with slate. Many black shale beds are essentially homogeneous, although under the microscope, a lamination by segregation of fine sericite flakes can be discerned. This layering at millimeter scale is metamorphic but undoubtedly reflects pre-metamorphic compositional layering of sediment. In some parts of the orebody small areas with low carbon content and of slightly bleached appearance consist of more micaceous phyllite, or chloritic phyllite (termed listwaenite or beresite in Russian terminology) but appear to be the result of local, late stage hydrothermal activity with little evident relationship to gold mineralization.

Bottom structures, such as load casts have not been found or reported, nor have cross-bedding, ripple drift or other internal structures.

All varieties of sedimentary rocks are metamorphosed to a minor variable degree, depending on the prior lithology. The mineral composition of the phyllites is monotonous and includes quartz (in large part clastic), sericite, siderite and carbonaceous material. Lesser minerals include ankerite, albite, chlorite, biotite, rutile, tourmaline and rarely clinochlore. With the exception of siderite all the metamorphic minerals are fine to very fine grained (to a few microns); siderite typically occurs as distinctly larger porphyroblasts (up to 4–5 mm in length) in the finer groundmass. The sizes of siderite porphyroblasts are more or less constant within individual thin carbonaceous shale beds but may vary markedly from one bed to the next. Furthermore the individual beds are commonly separated by wider intervals of non-sideritic carbonaceous shale, indicating their premetamorphic carbonate composition.

Three main varieties of host rock are recognized:

1. Quartz-carbonate-sericite carbonaceous shale, with 12–20% quartz, 40–70% carbonates mainly siderite-ankerite with lesser calcite, and 10–20% sericite. Carbonaceous material occurs as separate flakes up to 0.05 mm, usually from 0.1 to 2.1% but in some thin layers up to 5%. XRD analyses failed to detect graphite, while other tests failed to detect little more than a trace of bituminous compounds. A concentrate sample extracted from a large volume of carbonaceous phyllite was found to be similar to cannel coal [7]. The material is presumed to be mainly amorphous carbon, in spite of the low-grade greenschist facies metamorphism. However, recent intensive

microfossil research on samples from Dalnyaya Taiga (locality 12 in Fig. 3) and other localities in the Highlands strongly suggest a significant carbon input of biogenic origin (see later).

2. Siderite shales are characterized by plentiful and widespread siderite porphyroblasts at 40–60% of the rock volume, and they impart a coarser granular texture to the rock and a knotty irregularity to schistosity or cleavage surfaces. The preferential stratigraphic distribution of the carbonate porphyroblasts in shale beds and their absence from intervening psammitic strata strongly suggests original sedimentary-diagenetic control of carbonatization rather than a pervasive hydrothermal metasomatism.

3. Quartzitic siltstone or slate consists of more or less equigranular quartz grains about 0.1 mm with an admixture of sericite to around 10%, and ankerite to 5–10%. Siderite porphyroblasts are also usually present, but in small amounts.

Numerous quartz-carbonate inclusions, stringers, and veinlets are common in phyllite and shale, and frequently contain pyrite and other sulfides. They are internally impoverished in carbonaceous matter, which is in the form of fine flakes (0.005–0.007 mm) markedly concentrated along boundary zones. The inclusions and veinlets have a thickness from 1.5 mm to 6–7 mm in cross-section and consist of quartz and carbonate crystals of 0.2–0.5 mm, with pyrite aggregates of cubic and pentagonal-dodecahedral crystals.

A large number of whole rock analyses of phyllites within and outside the ore zone indicates considerable uniformity of chemical and mineral composition [7]. Semiquantitative spectral analyses of phyllite and quartz-carbonate shale revealed a consistent range of minor and trace elements, such as barium, chromium, zinc, manganese, strontium, lead, nickel, cobalt, copper, vanadium, scandium and beryllium, with arsenic and bismuth significantly absent (but present at low levels in ores).

Structure. The dominant structure of the locality is the regionally third-order Sukhoi Log Anticline, which encloses the deposit. It lies on the southern side of the regionally second-order Marakan-Tunguska Trough (synclinorium) with which it is congruent.

The Sukhoi Log Anticline is a large, reclining, nearly isoclinal flexural-slip fold with planar limbs and an acutely inflected hinge zone (Fig. 5). It developed synchronously with progressive low-grade greenschist facies metamorphism and is a typical first phase fold structure, designated F_1. The fold and the deposit it hosts constitute a GICSIAC (Gold in Carbonaceous Shale in Anticlinal Crest) in the terminology of Shields [13] but differs from most other anticlinal types in that the mineralization is essentially disseminated. Saddle reefs in intrastratal crests are almost entirely absent, and the penetrative axial schistosity and cleavage appear to have been the main conduits and locators of pervasive fluid movement.

The fold hinge zone is exposed for 3.3 km along the crest of Sukhoi Log hill (Figs. 1, *B* and 5) and the various structural elements change orientation to a small degree along strike. Near the west end the axial plane strikes at 295° and dips 25° NNE and the axis plunges 10–13° NW; in the central part the axial plane strikes 278°; its dip increases to 35° N and the axis plunges at around 8° WNW; near the east end, the fold is less acute, the axial plane strikes at around 270° and dips 38° N, and the axis plunges at 3–5° WNW.

Disseminated pyrite is evident in phyllite outcrops throughout the length of the anticline, but subsurface economic mineralization is developed only in the central part, with higher gold values mainly where the axial plunge is low [7]. The black shales throughout the fold have a penetrative axial plane cleavage, defined by oriented mica flakes. Also present at many places is a fine, close-spaced axially parallel lineation consisting of micro-crenulated mica.

Parasitic F_1 flexural-slip folds of second or third order to the main anticline are visible in underground drive walls, more especially in well-bedded strata (Fig. 6, *A*, *B*). They all have similar sinuous profiles and are congruent in each limb to the main anticline and to the main planar foliation and cleavage. Many include planar veinlets of high-grade quartz-pyrite-gold in their axial cleavages, and at some locations the fold limbs are offset or partially transposed across several close-spaced veinlets. In a few small F_1 fold-crests, quartz-pyrite-gold veinlets also occupy bedding plane openings in the manner of saddle-reef structures.

Other folds of small dimensions and more angular asymmetric profile are present but are less common. In these the main S_1 foliation and the associated schistose fabric are rotated by the shorter limbs. Also, an irregular axial plane fracture system may be developed especially where the hinges are more acutely inflected. These overprint the earlier generation of F_1 folds, and so occurred later in a different temperature-pressure regime as a separate phase of deformation (F_2). Many are intersected by or associated with small, high-grade quartz-carbonate-pyrite-gold veins of irregular, miniature saddle reef form and size (Fig. 6, *A*, *B*). They apparently developed under post-metamorphic conditions, but in a temperature range at which mineralizing fluids still remained mobile.

A later generation of small folds is also present as widely separated narrow zones of kink-bands (F_3) in which the bedding and foliation of phyllites are acutely inflected and fractured without development of quartz veining. The kink-bands (or short fold limbs) are generally subvertical with a northwestern trend, and are bounded

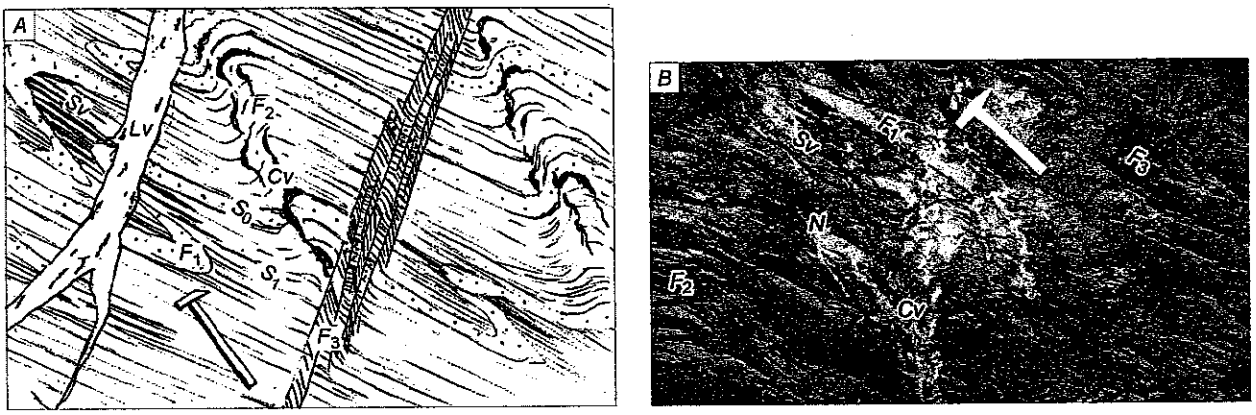

Fig. 6. *A* — **Composite structural scheme, showing small scale F_1 folds in bedding (S_0) with axial plane schistosity (S_1) and sheeted veinlets (*Sv*); F_2 folds in schistosity and bedding with contorted veinlets (*Cv*); F_3 kink-folds in bands of crumpling; late quartz-gold tensional vein (*Lv*).** *B* — **Photograph of Drive No. 1 wall, showing F_1 fold in bedding with sheeted veinlets (*Sv*), broad F_2 fold in bedding and schistosity, large pyrite nodule connecting with contorted veinlets (*Cv*), and zone of small F_3 kink-folds.**

on each side by a distinct irregular axial plane fracture. This generation may be related to a series of small left-lateral subvertical faults shown in Fig. 5, or possibly to two sets of quartz vein deposits striking at 320° and 285–290° reported by Kazakevich [3]. F_3 folds have little apparent effect on the widespread mineralization but may be brittle precursors to the fracture controlled late quartz-vein deposits, which represent the last low temperature stage of hydrothermal dewatering.

Faults. No major faults are known within the Sukhoi Log deposit, but one local fault underlies the alluvial deposits immediately along the south side of the Sukhoi Log ridge (Fig. 1, *B*). The fault does not separate major rock formations and occurs only within Patom Group strata.

Fifteen or more small parallel left-lateral faults are spaced along the length of the Sukhoi Log anticline. They strike at 340–350° (Fig. 6) and dip 70° E. Vertical displacement is negligible, and lateral offset is mainly less than 3 m.

Late quartz vein deposits. Two small quartz vein gold deposits on Sukhoi Log hill were mined in 1886 and 1894 but did not reach the gold-sulfide orebody below. A brief account of the work and results in the Sukhoi Log area was given by Kazakevich [3].

Other observers [7, 8] indicated that large subeconomic quartz veins of transgressive type are more numerous in the centre of the Sukhoi Log anticline, and constitute diagonal fracture fillings up to 3.5 m thick in the upper levels of the zone of mineralization. Several others are visible underground in other parts of the orebody, and are clearly later and transgressive (Fig. 6, *A*).

OREBODY FORM AND GRADE

The gold orebody has the form of an elongate lens of irregular plano-convex cross section within the disseminated pyrite envelope (Figs. 5 and 12), dipping northerly at 15–30°, with an irregular hanging wall and a more nearly planar footwall. The thickness at the 1 ppm cutoff is variable and ranges from 15 m at the concealed updip southern periphery to 140 m in parts of the interior. The upper edge of the orebody is 40 m below surface near the western end, and 60 m at the eastern end (Fig. 11). It extends down dip to more than 400 m and appears to be open to depth, and may also have significant extension in carbonaceous shale along the 13° NW plunge of the anticlinal axis.

Along the 2.2 km length of the C_1 category reserve, two lengthy thickened blackshale zones have developed where thinner stratiform units intersect the anticlinal hinge. These are consistently more than 100 m thick, with internal elongate flat lenses (termed ore pillars) of 4 ppm Au and up to 9.6 ppm (Fig. 12). The shallow southern zone at depths of 100 to 200 m, is 1.8 km long and 100 to 200 m wide. The deeper northern zone is 1.4 km long and 100 to 300 m wide at depths of 300 to 400 m. Konstantinov et al. [14, Fig. 6] provided an illustrative 3D diagram of the orebody grades at five 100 m levels and a gold-grade profile along Drive 2 in the lower anticlinal limb (Fig. 7).

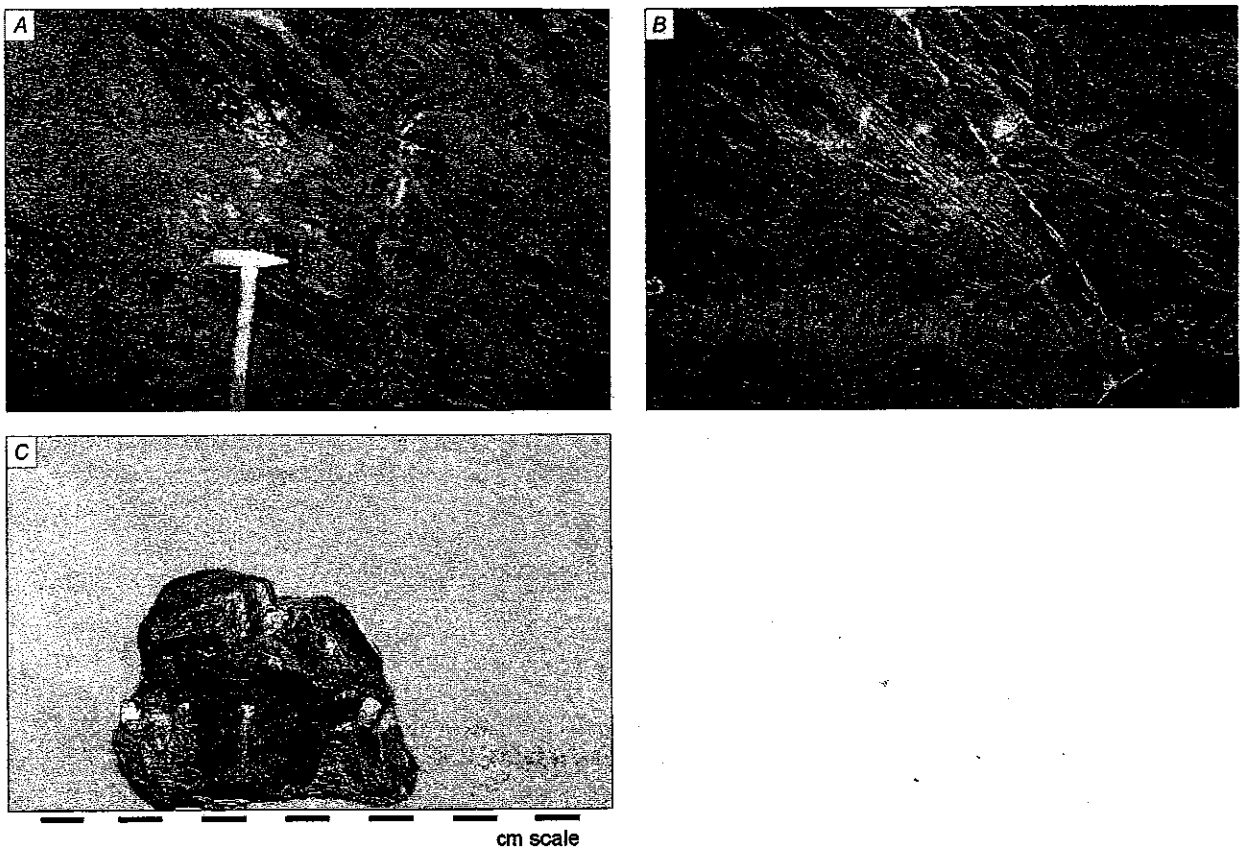

Fig. 7. *A* — Disseminated pyrite (Pyrite I). *B* — Sheeted veinlets, pyrite + quartz (Pyrite II). *C* — Porphyroblastic pyrite (Pyrite III).

MINERALOGY

Pyrite is distributed in three main modes, (1) disseminated, (2) lamellar or veined, and (3) porphyroblastic [5]. The first is widespread within and outside the ore zone and ranges from microscopic to 1 cm crystals in carbonaceous phyllite (Fig. 7, *A*). Lamellar irregular veins generally of small size are also widespread throughout the orebody, while sheeted veinlets (Fig. 7, *B*) are locally developed where phyllitic slate beds cross the hinge of F_1 anticlines, and are regularly spaced in concordance with the strongly penetrative axial-plane cleavage. Sulfide-quartz sheeted veinlets are typically 0.3 mm to 0.8 mm thick, with separation intervals of 1–4 cm, over several meters. Porphyroblastic pyrite occurs as large separate crystals, or as subidiomorphic clusters in specific layers or beds of black shale (Fig. 7, *C*). Their dimensions may reach 2–3 cm, and their gold content is considerably less than the other varieties.

A fourth much rarer mode comprises nodular crystalline pyrite as clusters of 1–2 cm "eyes" having elongated quartz pressure shadows forming the "corners" of the eyes, or even more rarely as lensoid aggregates up to 5 cm in length, comprising cores of crystalline pyrite surrounded by 1–2 mm framboidal spheroids in concentric layers. The texture is consistent with a low-temperature syndiagenetic sulfide product of bacterial activity (Fig. 8, *A*).

Additional ore minerals associated with pyrite but amounting to less than 2% of all sulfides include the following: pyrrhotite, chalcopyrite, scutterudite-chloanthite, sphalerite, galena, gersdorffite, millerite, pentlandite, violarite, rutile, magnetite. Sphalerite is the most common, locally to 3%. Traces occur of arsenopyrite, argentite, monazite, apatite and zircon.

Gold is distributed as separate grains up to 200 microns, in fractures in pyrite, at pyrite grain boundaries, and at pyrite-quartz boundaries. Most of the gold is associated with the pyrite and least with quartz.

Sulfide textures. Apart from the rare nodular pyrite of syndiagenetic bacterial origin mentioned above, the three main modes of disseminated pyrite are as follows (Fig. 7).

Pyrite I occurs as very finely disseminated idiomorphic cubic crystals and aggregates in phyllitic black shale

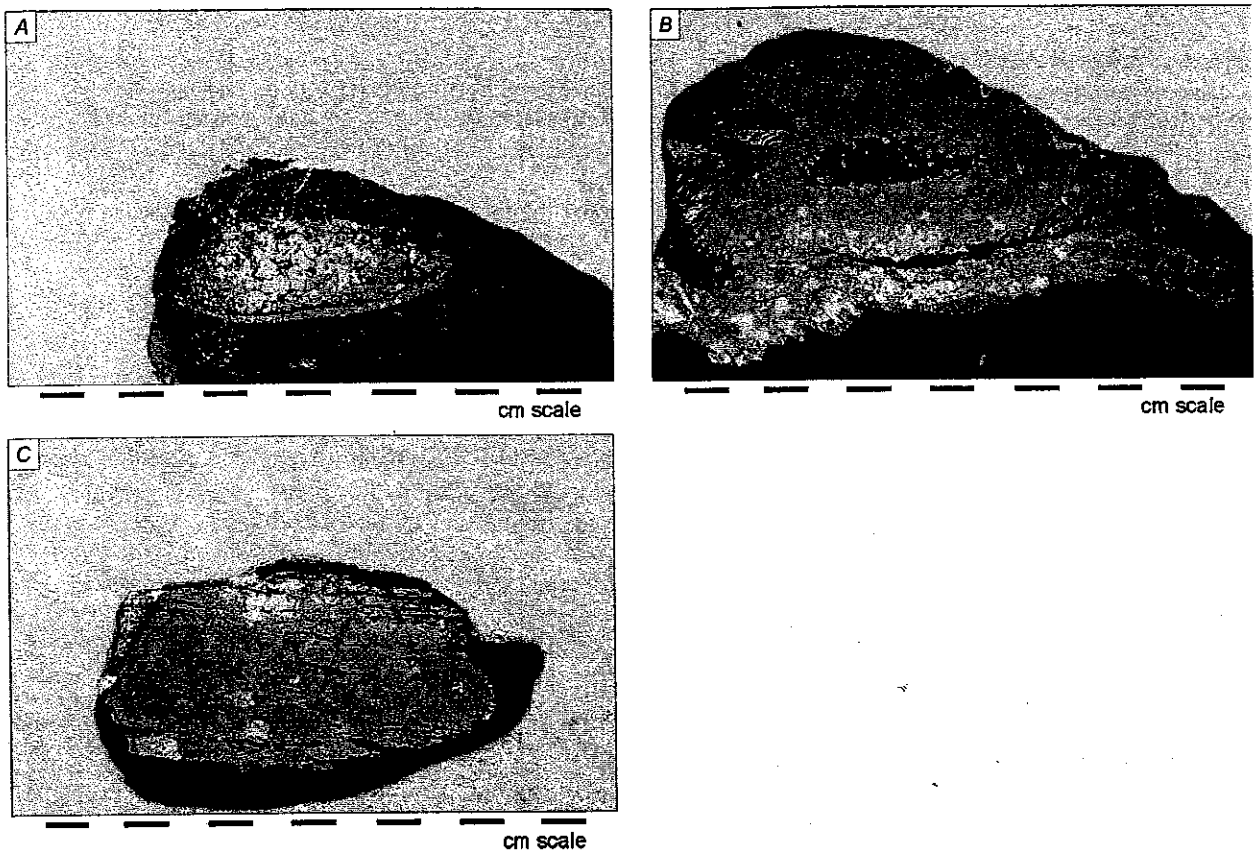

Fig. 8. ***A*** **— Large zoned nodule of crystalline pyrite rimmed by framboidal pyrite.** ***B*** **— Zoned nodule of crystalline pyrite, with quartz-pyrite-carbonate vein.** ***C*** **— Zoned nodule showing partial transposition with shale into layers.**

of the ore zone and in the surrounding envelope. The size of grains varies from 0.1 mm to 2–3 mm. The gold in pyrite content in the ore zone is 40 to 57 ppm. This pyrite is also widespread but of lower grade in the outer aureole of the ore envelope in the fourth and fifth Khomolkho subformations. It contains higher Ni and Co and lower As than other varieties. It also has widely dispersed $\sigma^{34}S$ values from –6‰ to +20‰, suggestive of a marine origin by bacterial sulfate reduction in a seafloor depositional environment [15]. Under the microscope a fine equigranular texture is evident, with some crystals enclosing a spherical pyrite core filled with fine disseminated carbon particles surrounded by an outer pyrite zone devoid of carbon inclusions and with a well-defined crystalline outline. This is also suggestive of a diagenetic origin for at least some of the pyrite, with the core corresponding to a bacterial spherule of initially amorphous sulfide and carbon, crystallized diagenetically, and then overgrown by later idiomorphic pyrite.

Pyrite II fills cleavages as sheeted or lamellar veinlets, and fractures where it forms small irregular veins (stringers). Pyrite II contains disseminations of the same materials as Pyrite I but their size is much smaller. The average gold content is 53 ppm (range from 27 to 203 ppm), and the silver content varies from 5 to 23 ppm. This pyrite contains higher As, and has more homogeneous $\sigma^{34}S$ values from +6‰ to +11‰, indicating a homogenized source [15], such as low greenschist facies metamorphic fluids.

Pyrite III is present in the form of single porphyroblastic well-formed crystals of up 1–2 cm in diameter or as clusters of large intergrown crystals (Fig. 7, *C*). The gold content is low from 0.1 to 5 ppm. It formed later than Pyrite I and Pyrite II as shown by enclosed pre-existing structures, lower temperatures of formation and composition of internal inclusions. Other elements in Pyrite III include higher As and lesser Ni than in the others, with a total absence of Cu.

Rare tectonized nodules of pyrite occur as boudins in zones of high competency contrast with interbedded sandstone and phyllite. Pyritic boudins have higher gold grades than adjacent ore, from 22 ppm to 113 ppm.

Pyrrhotite occurs in the shales, in quartz-pyrite veins and in Pyrite I and II. The form is isometric, irregular, drop-like. An association with gold is rare.

Chalcopyrite forms small aggregates in quartz veinlets. In shales and Pyrite I and II it is found together with the pyrrhotite as crystals from hundredths to tenths of a millimetre. Semiquantitative spectral analysis indicates that it contains silver. Sphalerite is in separate grains with galena and chalcopyrite in quartz veins and quartz-sulfide veins.

Galena is rarely present, in the form of single grains up to 0.2 mm in pyrite, chalcopyrite and sphalerite, or with gold and quartz.

Arsenopyrite forms scarce idiomorphic grains 0.1 to 0.3 mm, in quartz and pyrite. Other sulfides are rare and are in the form of small single grains. Argentite is very rare and is associated with chalcopyrite.

MODE OF OCCURRENCE OF PRECIOUS METALS

Gold. Gold is present only in pyrite or quartz-pyrite-carbonate veins. It reaches highest values in sheeted veinlets (50–200 ppm in pyrite), and has overall low values in Pyrite III (around 5 ppm in pyrite). Gold of economic or geochemically anomalous concentrations is absent from black shale that lacks pyrite.

Two genetically different types of gold are recognized in the deposit and differ in purity. The purer gold (900–920 fine) is in minor drop-shaped particles inside pyrite crystals associated with other sulfides or quartz. Such gold is thought to be syngenetic within metamorphogenic pyrite, and to have formed primarily by droplet enlargement of original very fine dispersed gold within formerly syndiagenetic pyrite [15], as in the carbonaceous spherulitic cores of some Pyrite I crystals. The less pure gold (840–880 fine) was deposited later as coarser grains in veins and sheeted veinlets, with Pyrite I and II and quartz, and has undergone limited hydrothermal translocation and contamination by other metals. The relative abundances of the three modes of typical gold occurrences are shown in Fig. 9, *A–C* and in Table 1.

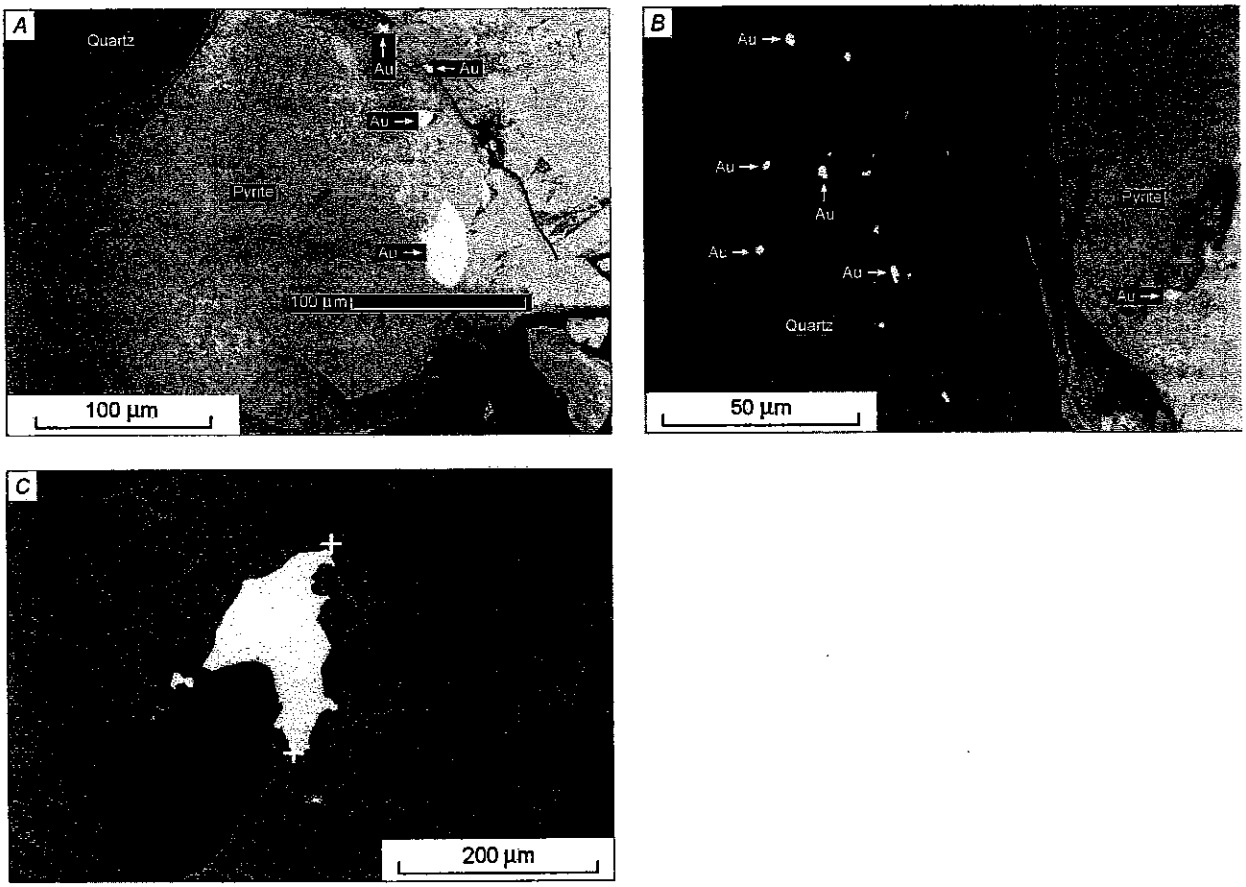

Fig. 9. ***A*** **— Coarse gold included in pyrite.** ***B*** **— Gold in quartz adjacent to pyrite.** ***C*** **— Coarse gold at pyrite-quartz boundary.**

Table 1

Modes of Occurrence of Gold

Association*	Sample					
	M2	M3	M8	Average	Gravity concentrate	Flotation concentrate
Locked in pyrite	95.7	87.8	66.0	83.2	9.4	12.0
Locked in gangue	—	—	2.4	0.8	—	—
Grain boundaries	4.3	12.2	31.6	16.1	14.4	9.4
Liberated	—	—	—	—	76.2	78.6

Gold Particle Size Distributions (vol.%)

Grain size, μm	Locked in pyrite	Locked in gangue	Interstitial between pyrite grains
	93.3	5.6	1.2
<10	5.8	73.2	100
10–20	17.1	26.8	—
20–30	16.0	—	—
30–40	16.5	—	—
40–50	44.6	—	—

*** Relative volume percentage.**

Grain-size data on gravity and flotation concentrates show that a significant amount has diameters more than 40 microns, and only a small amount less than 10 microns (Table 1).

Within Pyrite I and II some gold grains are located in or alongside small grains of quartz, pyrrhotite, chalcopyrite, galena, and sphalerite. In gangue minerals some gold grains are free and others are associated with the aforementioned sulfides. Gold was deposited from ore fluids with these lesser sulfides, and so overlapped the late stage of Pyrite I and II, and was almost completed by the first stages of Pyrite III, which has low gold content. Within sheeted veinlets, and in disseminated pyrite, the gold is associated mainly with Pyrite I, and in quartz-pyrite veins it is mainly with Pyrite II. Early gold grains in pyrite and gangue tend to be compact in shape, later grains tend to be elongate, platy or wirelike as if formed in cracks and grain contacts of fully crystallized host minerals (Fig. 10, *B*).

Silver. Silver occurs in variable amounts as argentite in other sulfides and as an alloy with gold. Silver content in some assays exceeds that of gold, but there is no direct correlation between them, and overall the gold-silver ratio is in the order of 7:1, equivalent to a gold fineness of almost 880.

Platinum and PGM. Limited preliminary analytical results obtained in 1996 as part of the feasibility study of Sukhoi Log confirmed platinum and other PGM presence, like those previously reported from other Russian localities [16]. More recent research [17, 18] has considerably enlarged the mineralogical and paragenetic database of these and other metals.

Sequence of crystallization. An early syndiagenetic development of nodular pyrite is indicated by the few larger nodules discovered to date, and was probably accompanied by a contemporaneous widespread development of precursor diagenetic sulfide phases such as greigite and mackinawite. Following sediment compaction and crystallization of precursor sulfides into microcrystalline pyrite [19], dispersed iron carbonates generated by catalytic auto-oxidation of biogenic sedimentary carbon [20] also began to crystallise as siderite at the onset of regional metamorphism, and continued as the main phase of folding and deformation ensued. Thus some porphyroblasts of siderite enclose shale relics with phyllitic texture and very fine grained sericitic mica.

First generation disseminated pyrite (Pyrite I) began crystallizing after the main siderite porphyroblasts, and some pyrites enclosed already existent siderite crystals. These are now preserved as remnant fragments inside pyrite crystals, and show their original crystal unity by simultaneous extinction under the microscope. The high grade

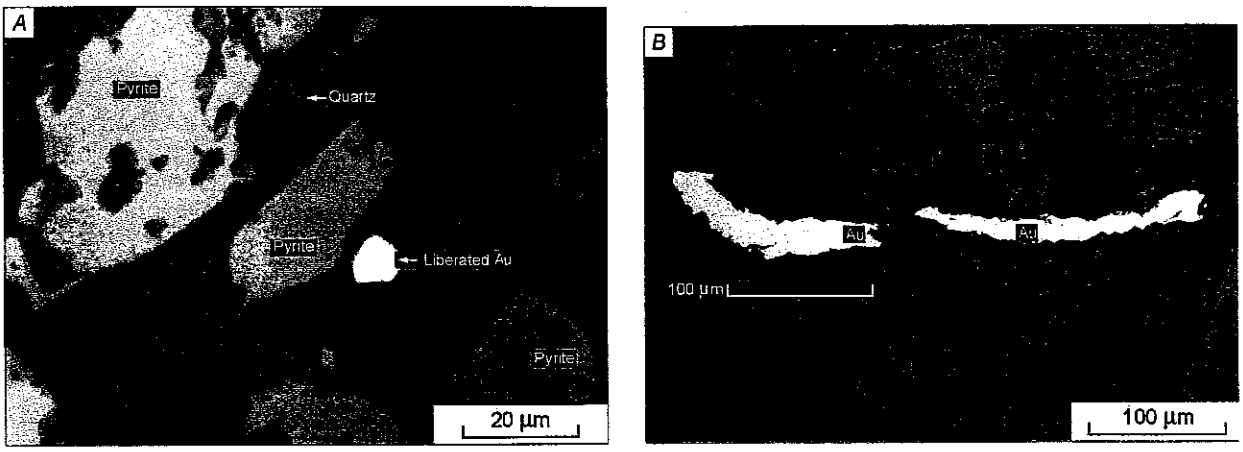

Fig. 10. Form of gold grains. *A* — Liberated gold in flotation concentrate. *B* — Coarse gold particles in gravity concentrate.

and purity of gold within first generation pyrite implies that the metal must have been available in disseminated form in the black shale matrix from the onset of pyrite crystallization [21], as does the occurrence of other native accessory elements such as PGM, Cu, Fe, Cr, W, Ti [22]. This phase of Pyrite I development was thus syn- to late-metamorphic, by which time deformation was well advanced, with an axial plane schistosity containing Pyrite II lamellae beginning to develop in the Sukhoi Log anticline. Possibly some growth of sheeted veinlets in axial cleavages also occurred at the same time.

As this process continued, Pyrite II with lesser quartz and the carbonates, ankerite and dolomite, began to dominate the veinlet assemblage, and to develop clustered and isolated thin transgressive quartz-gold-carbonate and quartz-gold veins (Fig. 8, *B*). Siderite porphyroblasts are cut transgressively by Pyrite II veinlets, indicating the younger age of the latter. During this stage the minor accessory base metal and platinum group sulfides developed under conditions of increasing sulfur activity [22], and some of the elements were incorporated in gold, resulting in the lower fineness of Pyrite II gold.

The sequence of sulfide mineralization terminated with crystallization of Pyrite III, mainly as single large porphyroblasts in black shale or less commonly as crystal aggregates (Fig. 7, *C*) with little or no quartz or deformation features. These transgressively intersect all other pyritic structures and related quartz veins. Also noteworthy is their consistently lower grade of contained gold (<10 ppm as against >10 ppm for Pyrite I and II), the higher As content and the absence of Cu.

It should be noted here that Pyrite III of this account is a later generation than that of Korobeinikov et al. [18, p. 437–438] which is a clustered-stringer type containing Pyrite II of this account.

RESERVES AND RESOURCES

The geological limits of the envelope of mineralization and the boundaries of productive zones are entirely dependent on the intensity of sulfide mineralization. During evaluation drilling in the 1970s this provided the basis for defining and sampling ore in drill cores, and with few exceptions proved a reliable criterion in the light of the many systematic checks on results that were made by the various Russian authorities during the progress of evaluation work and later.

The system for estimating Russian ore reserves and resources was based on established, well defined specific rules and regulations with many balances and checks. It was widely applied throughout the former Soviet Union and underwent six major revisions since initiation in 1927 [23].

In the context of the Russian system of reserve-resource definition, the categories shown in Table 2 and Figure 11 are approximately equivalent [23] to Proven/Probable Reserves (B), Measured/Indicated Resources (C_1 and C_2), and Inferred Resources (P) of the Australasian JORC Code (1996). In terms of the U.S. system they are equivalent to Measured/Proved Reserves (B), Indicated/Probable Reserves (C_1), Inferred/Possible Resources (part C_2 and P_1).

In addition to Sukhoi Log, Table 2 includes the two small satellite deposits Radostny Central and Zapadny, and three more distant deposits of the same type (for locations see Fig. 2). The Sukhoi Log tonnages are those of

Table 1

Modes of Occurrence of Gold

Association*	Sample					
	M2	M3	M8	Average	Gravity concentrate	Flotation concentrate
Locked in pyrite	95.7	87.8	66.0	83.2	9.4	12.0
Locked in gangue	—	—	2.4	0.8	—	—
Grain boundaries	4.3	12.2	31.6	16.1	14.4	9.4
Liberated	—	—	—	—	76.2	78.6

Gold Particle Size Distributions (vol.%)

Grain size, μm	Locked in pyrite	Locked in gangue	Interstitial between pyrite grains
	93.3	5.6	1.2
<10	5.8	73.2	100
10–20	17.1	26.8	—
20–30	16.0	—	—
30–40	16.5	—	—
40–50	44.6	—	—

*** Relative volume percentage.**

Grain-size data on gravity and flotation concentrates show that a significant amount has diameters more than 40 microns, and only a small amount less than 10 microns (Table 1).

Within Pyrite I and II some gold grains are located in or alongside small grains of quartz, pyrrhotite, chalcopyrite, galena, and sphalerite. In gangue minerals some gold grains are free and others are associated with the aforementioned sulfides. Gold was deposited from ore fluids with these lesser sulfides, and so overlapped the late stage of Pyrite I and II, and was almost completed by the first stages of Pyrite III, which has low gold content. Within sheeted veinlets, and in disseminated pyrite, the gold is associated mainly with Pyrite I, and in quartz-pyrite veins it is mainly with Pyrite II. Early gold grains in pyrite and gangue tend to be compact in shape, later grains tend to be elongate, platy or wirelike as if formed in cracks and grain contacts of fully crystallized host minerals (Fig. 10, *B*).

Silver. Silver occurs in variable amounts as argentite in other sulfides and as an alloy with gold. Silver content in some assays exceeds that of gold, but there is no direct correlation between them, and overall the gold-silver ratio is in the order of 7:1, equivalent to a gold fineness of almost 880.

Platinum and PGM. Limited preliminary analytical results obtained in 1996 as part of the feasibility study of Sukhoi Log confirmed platinum and other PGM presence, like those previously reported from other Russian localities [16]. More recent research [17, 18] has considerably enlarged the mineralogical and paragenetic database of these and other metals.

Sequence of crystallization. An early syndiagenetic development of nodular pyrite is indicated by the few larger nodules discovered to date, and was probably accompanied by a contemporaneous widespread development of precursor diagenetic sulfide phases such as greigite and mackinawite. Following sediment compaction and crystallization of precursor sulfides into microcrystalline pyrite [19], dispersed iron carbonates generated by catalytic auto-oxidation of biogenic sedimentary carbon [20] also began to crystallise as siderite at the onset of regional metamorphism, and continued as the main phase of folding and deformation ensued. Thus some porphyroblasts of siderite enclose shale relics with phyllitic texture and very fine grained sericitic mica.

First generation disseminated pyrite (Pyrite I) began crystallizing after the main siderite porphyroblasts, and some pyrites enclosed already existent siderite crystals. These are now preserved as remnant fragments inside pyrite crystals, and show their original crystal unity by simultaneous extinction under the microscope. The high grade

Table 2

Reserves and Resources, Primary Gold, Lena-Bodaibo Goldfield

Deposit	Russian mineralization category	Million tonnes	Grade (ppm)	*In situ* gold (million oz)	Strip ratio (waste per t ore)
Sukhoi Log					
	B	52	2.5–2.7	4.2–4.5	3.7
In pit	C_1	199	2.5–2.7	16.0–17.3	3.7
	C_2	133	2.5–2.7	10.7–11.5	3.7
Subtotal, pit	—	384	2.5–2.7	30.9–33.3	3.7
Pit extension	Low grade	205	0.8	5.3	0
	C_2	165	2.0–2.3	10.6–12.2	7.0
Total Sukhoi Log	—	754	1.9–2.1	46.8–50.8	3.4
Radostny*	C_2+P_1	2.0	6.3	0.42	6.0
Tsentralny	P_1	8.0	4.5	1.20	
Radostny	P_1	4.6	5.0	0.74	
Zapadny	C_2+P_1	5.3	3.5	0.60	8.0
Subtotal with Sukhoi Log	—	14.6	4.9	2.4	—
	C_1+C_2	21	2.9	2.0	3.0
Verninsky	Low grade in waste	10–20	0.5–1.6	0.5	0
Pervenets	C_1	0.8	5.3	0.1	16
Vysochaishy	C_2	15	3.0	1.5	2.5
Total	—	820	2.0–2.2	53.3–57.3	—

*** Mined with Sukhoi Log.**

the consultant mining and pit design group, VNIPIPromtechnologii (All-Russian Designing and Research Institute of Production Engineering). IRGIredmet (Irkutsk Research Institute of Precious Metals) also estimated similar tonnages in an earlier pit design. The information on the five lesser deposits is based on exploration archives held by the Bodaibo Geological Expedition, which performed most of the exploration in previous years.

MODE AND SEQUENCE OF ORIGIN

Although disseminated gold-PGM mineralization in black shale has long been known at many places, such as Lyublin, Poland [20], southeastern China, Canada and U.S.A. [21], many of the host rocks are thin extensive platform sediments of limited accessibility for mining. More recently, anomalous levels of PGM are being reported in increasing numbers of gold deposits and mines in marine flyschoid carbonaceous shale-hosted deposits of Russia, Ukraine, Kazakhstan, [16–18, 24, 25], in bitumen at the Boss Mine, Nevada [26], and in the Magdala mine in Victoria, Australia (see later).

Sukhoi Log may be one of the largest and probably the first major disseminated gold-PGM deposit to be discovered in marine carbonaceous shales, and some discussion of its mode of origin may provide a model for other discoveries of the same kind.

As outlined earlier, the regional geological setting of the Sukhoi Log and the five lesser black shale disseminated deposits of the Lena goldfield is that of a complex folded sedimentary sequence at the exposed northeastern end of the Akitkan Foldbelt and the included Olokit Zone, parts of both of which extend into the western side of the goldfield area as shown in Fig. 3 [12, 27].

The Foldbelt is the only terrane within the Siberian Craton that is not underlain by Archean basement [27, p. 413]. It is interpreted [28] to have been a Lower and Middle Proterozoic oceanic basin sequence (1800–1600 Ma)

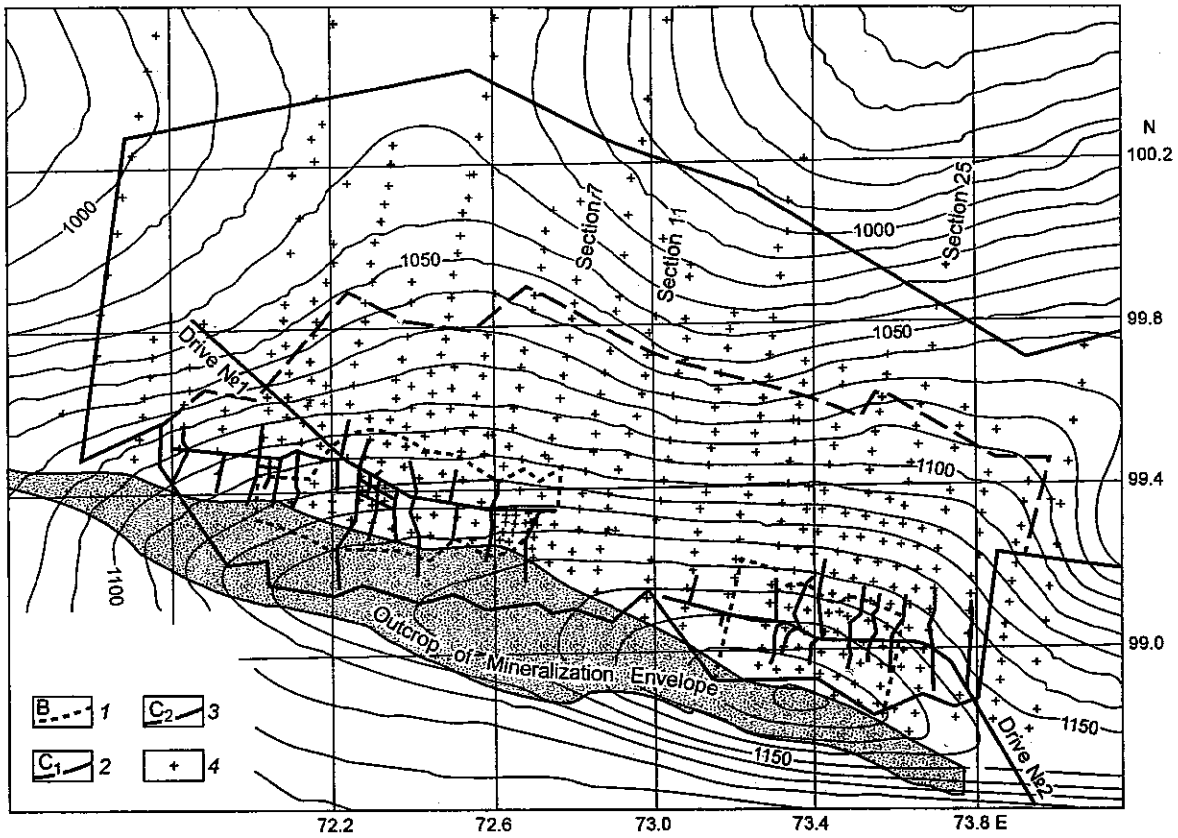

Fig. 11. Plan of Sukhoi Log orebody, showing Drives Nos. 1 and 2, drillhole locations and outcrop of the low-grade mineralization envelope. *1–3* — orebody categories, *4* — drill hole localities.

that was closed and underwent metamorphism in Late Precambrian–Riphean time (650–570 Ma) during Aldan-Magan collision, at the end of the Baikalian tectono-mągmatic cycle [5, p.8]. Recent advances in micropaleontology [29–31] and regional mapping have enabled correlation of the Patom Highland stratigraphic sequences with those further south in the Muya district (near Taksimo in Fig. 2) of oceanic and island arc origins [32–35] and confirm the variety and extensive Precambrian unity of the Akitkan Foldbelt.

In the Muya district, the Foldbelt is a Lower to Middle Proterozoic marginal-sea accretionary assemblage of oceanic island volcanics, ophiolite (i.e. oceanic crust) [36, 37] and subduction related intrusives and eruptives. Within the younger, 20–25 km wide Olokit Zone along the southeast side of the older accretionary complex, part of the sequence resembles that of the Patom highlands but also includes differentiated volcanic sequences up to 2 km thick. Graphitic flyschoid black shale hosts the large Kholodninskoye stratiform sulfide Pb-Zn deposit, in which lead isotope data indicate an initial synsedimentary-exhalative (sedex) origin of the same age as the host rocks (740±10 Ma), followed by metamorphic remobilization in the Riphean interval of 600–550 Ma [12].

Several lesser deposits are also known in the Olokit Zone, including barite-polymetallic types in carbonate rocks, copper-nickel mineralization in the Dovyren layered intrusives and Avkita meta-ultramafites, and banded silica-iron formations in Tyya and Medvezh'ya greenschists (Fig. 3), all of which have indications of rift-basin origin in the interval 1050–700 Ma [12]. As in parts of the Akitkan accretionary assemblage, the rocks in the Olokit Zone underwent several episodes of folding, of kyanite-sillimanite zonal metamorphism and regression, of superimposed thrusts and reverse faulting.

The similarity of the Riphean sedimentary sequences in the Patom Highlands to those of the Olokit Zone and to other parts of the Akitkan Foldbelt reinforces direct correlation and the demonstrable continuity (Fig. 3) between the gold-bearing, folded, low-grade greenschist facies metamorphics of the Patom Highlands with the PbZn-bearing intensely deformed, higher-grade kyanite-sillimanite Olokit metamorphics of the accretionary Akitkan Foldbelt.

In this structural context the contemporaneous but less deformed metavolcanics and metasediments of the

Patom Highlands are interpreted to have been deposited in part of the Olokit marine rift basin contiguous with the Akitkan sea, but also partly overlapping onto an epicratonic shelf at the western edge of the Aldan Shield, represented in the southeast Highlands by a condensed sequence overlying Archean Chara units (Figs. 3, 4, and 14, *B*). This interpretation further implies that Riphean subduction and accretion of the Akitkan-Olokit oceanic sediments was westerly, and occurred either at the Vilyui Fault (Fig. 3), or at the major geophysically defined but concealed Lena Fault Zone [27].

Tectonic sequence. The ages of many of the foregoing events are well constrained by a variety of isotopic data, some of which also have relevance for the origin of the disseminated gold deposits of the Sukhoi Log type.

These include (1) contents of the main Akitkan Foldbelt, 1800–1600 Ma, Lower Proterozoic PR_1, [28]. (2) metaporphyries at the base of the Olokit Group of the Foldbelt, 1863±5 Ma [4], (3) Pb isotopic model ages of the Kholodninskoye Pb-Zn sedex deposit in the middle of the Group, 740±10 Ma, Upper Proterozoic PR_3 [12], (4) the Dovyren layered intrusion in the middle of the Group, by three different methods, 700±20 Ma [38], (5) metaporphyries at the top of the Group, 700±20 Ma Upper Proterozoic PR_3 [39]. All these range from Lower Proterozoic to Upper Riphean (Late Precambrian) in age and all predate the final collision and closure of the Akitkan ocean. The ensuing regional metamorphism that followed closure occurred in the range of 600–550 Ma, as indicated by the Rb-Sr method on Kholodninskoye host metapelites, and by the Sm-Nd method on garnet amphibolites [12].

The geology and isotope data of the Kholodninskoye and several lesser sedex polymetallic deposits in the Olokit Group have been interpreted by several workers as indicating a rift basin environment now preserved as the accreted Olokit-Mama paleorift trough [40]. Similar interpretations but with varying emphasis on metamorphic, hydrothermal, and epithermal aspects have also been proposed by previous observers for the origin of the Sukhoi Log and other disseminated gold deposits of the Highlands, although from less evidence. However, extensive Pb isotope data [12, Fig. 148] indicate that all the varieties of gold in the Lena field, from disseminated, to vein, to placer types have identical Pb isotopic compositions. This may indicate just one original gold source for all the modes of occurrence, the earliest of which at Sukhoi Log was premetamorphic and synsedimentary.

The recent discovery of platinum group metals in and above the Sukhoi Log ore zone has further implications of a contemporaneous mantle-type primary source of the metals [18, p. 437], and subsequent synsedimentary deposition overlapping that of the gold.

Thus the later evolution of the Akitkan Foldbelt changed from that of a major collisional-subduction system to include a lengthy rift basin along its eastern side (Fig. 13). Within the regional basin terrigenous molasse type conglomerate, sandstone and limestone alternated with carbonaceous sediments as indicated by the stratigraphy in Fig. 4, in ephemeral locally deeper anoxic basins, analogous to the Atlantis II Deep in the present Red Sea. The main rift basin is now the accreted Olokit-Mama Zone with its sedimentary-exhalative Pb-Zn mineralization, and the epicratonic extension is the Patom Group in the Highlands with its seafloor hydrothermal-exhalative Au-PGM mineralization. The changeover probably began at about 1350 Ma (mid-Proterozoic) but was undoubtedly a lengthy process.

Rift basin origins. Exhalative metal precipitates are now known in a variety of geological environments on the modern seafloor [41] and include mid-ocean ridges, axis and off-axis seamounts, back-arc spreading centres, and sedimented intercratonic rifts. Examples of the latter type are (a) the Red Sea, in which density-stratified metal-rich brines overlie mineralized sediments in the Atlantis II Deep with average values of 0.6 ppm gold and up to 5.6 ppm gold (b) the Gulf of California within which Guyamas Basin seafloor sediments are mineralized with low gold and up to 350 ppm Ag, north of which the spreading zone of the East Pacific Rise intersected and rifted the continental edge, and (c) the Middle Valley and Escanaba Trough on the northern end of the East Pacific Rise where sulfide sediments are actively forming with mainly low gold contents <0.2 ppm and up to 2 ppm, beyond which the spreading zone extends beneath the North American continental edge. These examples demonstrate that an oceanic spreading ridge may provide a source of exhalative gold and other metals that can be mobilized by oceanic crustal rifting during subductive collision with a continental edge.

Thus the advent of the Olokit rift basin along the eastern side of the much older, orogenically convergent Akitkan belt is inferred to have been the result of the collision of a formerly median oceanic spreading ridge with the eastward encroaching Akitkan subduction zone. In the early stage of MOR subduction the leading limb of the spreading ridge would be undergoing compressional effects but as the central ridge enters, a slab window will open and bring hot asthenosphere into contact with the base of the cold wet accretionary prism [42]. Thermal effects would include uplift, localized high-*T* low-*P* metamorphism, local intrusion of plutons, and possibly orogenic gold-quartz vein deposits in the overriding edge. At a later stage the much slower trailing limb with its array of normal faults in the downbending lithosphere [43] would undergo extensional effects by slab pull [42, p. 48], including deep basin-margin rift faulting of oceanic crust in front of the subduction zone. This much longer-lived

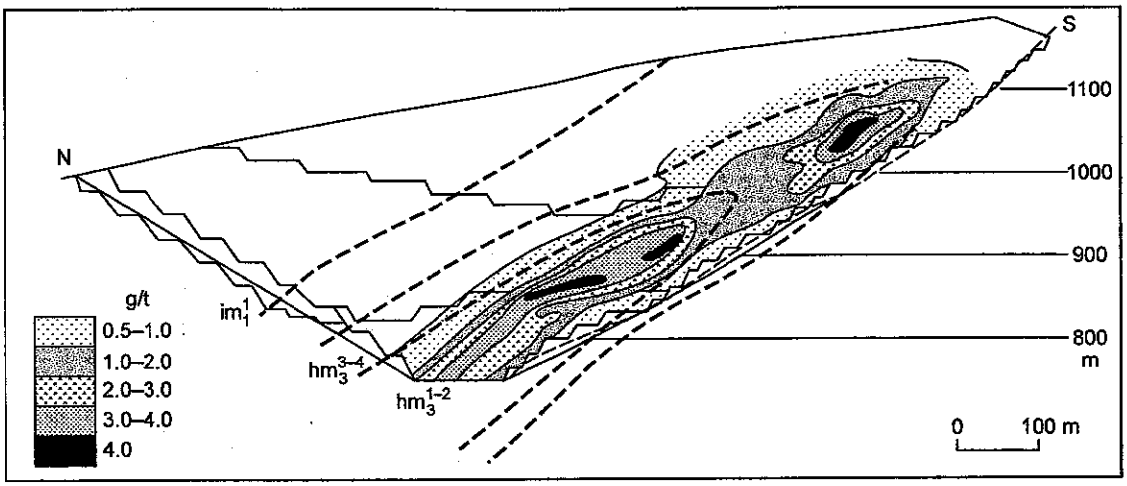

Fig. 12. Section +25 through the orebody showing higher-grade gold zones (ore pillars).

phase of slower trailing limb subduction would allow emission of crustal and mantle-sourced komatiitic or deeper hydrothermal fluids (not necessarily volcanic) carrying gold and PGM directly into the marine environment (Fig. 16, *B*) along a considerable length of the zone and trench, and probably spreading widely across the basin. A connection with ridge subduction and gold mineralization has been reported in Alaska [44], and another possible example with gold and reportedly low-level platinum group elements may occur in the Magdala gold mine at Stawell in western Victoria, Australia [45].

Ridge subduction has probably occurred more frequently in the geological past than has yet been recognized, in that almost every former oceanic closure involved either shutdown (death) of a spreading ridge, or subduction (burial) of an active one with some degree of rift faulting and seafloor exhalative mineralization prior to closure. Following Sisson and Pavlis [46, p. 913], "the history of any ocean basin must at some point in time include three plate interactions such as subduction of oceanic ridges, transforms or trenches. The resultant triple-junction interaction should lead to a distinct geological event in the fore arc of the plate margin. Yet consequences of this interaction remain one of the most poorly understood geologic phenomena."

Post-rift closure and metamorphism. Convergence of the Aldan and Magan basement blocks finally closed the oceanic Olokit rift system and resulted in synmetamorphic deformation of sediments in the Zone and the present Highlands during the Riphean (600–550 Ma). The metamorphism and deformation in the Olokit Zone is intense, with retrogressed fault-slices of granulitic basement and isoclinally folded kyanite-sillimanite metasediments [12]. In contrast, the adjoining Patom Group sediments were metamorphosed only to low-grade greenschist facies, and were coherently folded under ductile conditions. This difference is attributed to the existence of an underlying resistant basement shelf of the Aldan Shield, on which the Patom Group sediments were deposited and later tectonically stacked by marginal thrusting southeastward during the later stages of Olokit basin closure (Fig. 14, *C*).

The early stages of greenschist facies metamorphism in which clays change to white mica ± chlorite, generate considerable volumes of low-salinity fluids [47] that can mobilize initial sulfide phases in carbonaceous sediments, such as griegite, mackinawite, and amorphous bacterial sulfide into crystalline pyrite. Gold, platinum group and many other metals that may initially be present in a variety of organometallic compounds [20] or as thiol complexes [41] are also converted to inorganic crystalline phases and native metals [17] during the clay–sericite transition. As pressure–temperature conditions increase many of the initial phases recrystallize and change in form or composition, simulating a later paragenesis.

In the initially premetamorphic proto-Sukhoi Log deposit, the mineralization was probably spread at low concentration over a large area of anoxic seafloor in a locally deeper Olokit rift basin. Carbonaceous mud containing thermochemical and bacterial sulfur is capable of sequestering gold and other metals from density stratified brines after sufficiently long residence time, to near economic quantities and values [41] as are certain bacteria [48]. Many metals may initially form organometallic compounds under such conditions, [20] so that they become entrained in highly dispersed form. At an early stage of diagenesis the compounds may polymerize in kerogen, crystallize as metallocenes, or reduce to low-temperature sulfides such as greigite and mackinawite, marking the end of the syngenetic stage.

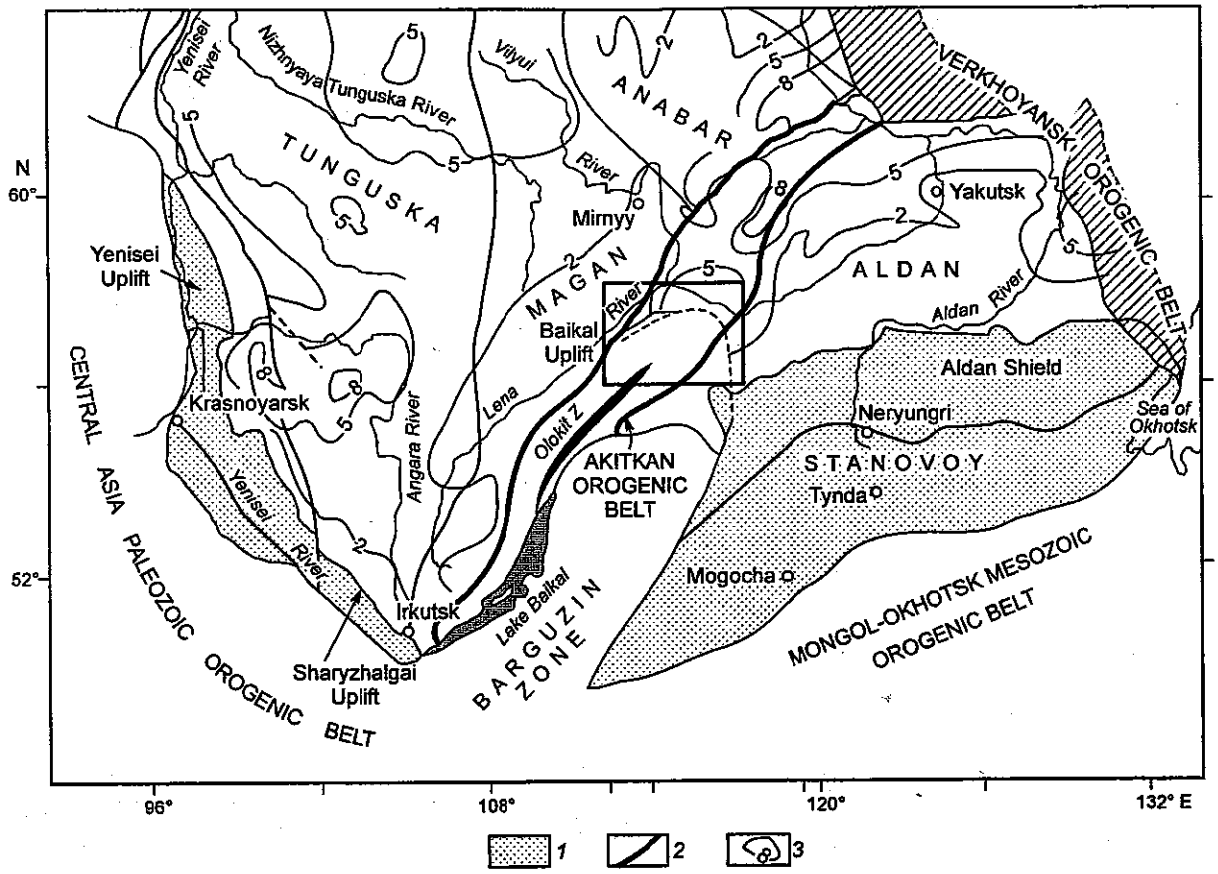

Fig. 13. Regional cratonic setting of the Patom highlands and Lena goldfields, showing the Akitkan Orogenic Belt and the Olokit Zone within it [27]. The rectangle represents the area of the Geological Map, Fig. 3. *1* — areas of major outcrop, *2* — main sutures, *3* — thickness of platform sediments (contours in km).

Synmetamorphic deformation of the Patom Group generated an initially southeast facing array of two major synclinoria, Bodaibo-Vitim to the southeast and Marakan-Tunguska to the northwest, separated by the Kropotkin anticlinorium which includes the present south-facing Sukhoi Log anticline. Metamorphism occurred beneath a tectonically stacked cover of probably 7 km or more of Patom Group sediments, and at a temperature of around 350 °C [49]. Metamorphic fluids were derived within the brittle-ductile transition zone from the large source volumes in the limbs of the anticline, and similarly in the smaller anticlinal Vysochaishy deposit 35 km to the northeast. Once liberated, the fluids scavenged disseminated metals including gold and platinum, and were driven by powerful tectono-dynamic pressure gradients [47] generated by tectonic thinning of the fold limbs and thickening of pelitic strata in the fold hinge. Development of a penetrative axial plane cleavage (S_1) allowed passage of fluids through psammitic strata, imparted considerable permeability to pelitic units and focussed greater volumes into the hinge zone. The carbonaceous composition of the pelitic strata undoubtedly constituted a reductant chemical trap at this stage for the metals in solution, and so gold accumulated in the tectonically thickened crestal zones to form the two major higher-grade "ore pillars" along the anticlinal axis (Fig. 12). The higher gold grades there also indicate preferential mobilization of gold in solution from limb regions and redeposition in the axial zones, as is reported from the Homestake Mine [50]. In addition, the overlying Imnyakh limestones may have functioned as a less permeable structural trap and so enhanced metal accumulation in the upper levels of the anticlinal crest. Near-closure of the anticline by penetrative flexural slip folding (F_1) completed the main synmetamorphic stage of evolution of the deposit.

Continuing deformation under decreasing stress and probably depth, generated the small F_2 nonpenetrative flexural folds with their associated contorted veinlets Post-metamorphic uplift and crustal extension subsquently developed the large, tensional quartz-gold veins, which although of uniformly low grades, sourced most the historic alluvial deposits of the Lena goldfield region.

In some respects the early stages of origin of the Sukhoi Log deposit seem similar to those of the recently

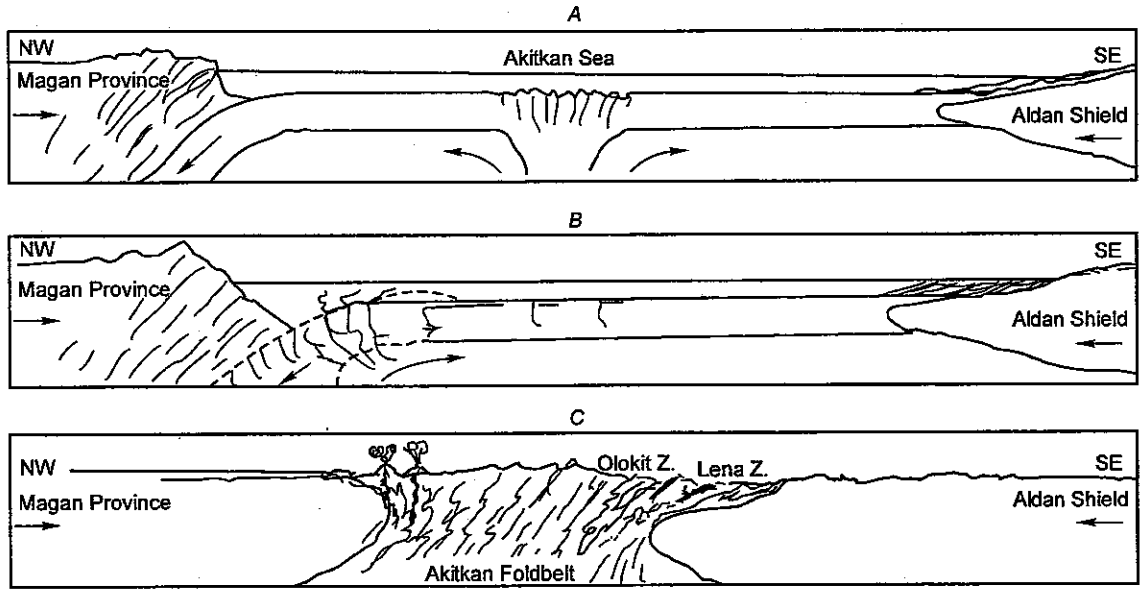

Fig. 14. Serial diagrammatic cross-sections NW-SE across the Patom highlands area depicting stages of development of the Akitkan Foldbelt and Sukhoi Log gold deposit. *A* — The Magan Province and Aldan Shield are converging with subduction under the Magan Province; the Akitkan Sea with its MOR spreading zone and the Aldan Shield are together moving to the subduction zone. 1800–1300 Ma. *B* — Collision of the MOR with the subduction zone is followed by rifting of the oceanic crust of the trailing limb, resulting in hydrothermal emission of deep-sourced crustal and lithospheric mantle fluids through extensional faults in front of the subduction zone. These generate exhalative Au-PGM mineralization of seafloor sediments in anoxic rift basins, the nascent Olokit-Lena deposits. 1300–600 Ma. *C* — Subduction has almost closed the Akitkan seaway. The Olokit anoxic basinal and terrigenous molasse deposits are thrust against the Aldan margin to form the Olokit Zone and partly onto the margin to form the syndeformational, synmetamorphic Sukhoi Log and other deposits of the Lena Goldfield (600–550 Ma).

discovered sedex gold deposits underlying the Carlin field, Nevada, [51, 52] in that both may have been generated by crustal rifting.

The final stage of regional deformation of the Patom Highlands was probably due to transpression by southward drift of the Aldan Shield which caused the regional oroclinal bending [53] of all the major structures into the unique semicircular regional pattern shown in Fig. 3. This probably occurred during development of the F_3 kink-band folds in the Sukhoi Log shales, and prior to emplacement of the northeasterly rectilinear zone of basic and lamprophyric dikes dated at 313±59 Ma [36], that is, between Late Riphean and Late Carboniferous. Although attributed by Zohnenshain et al. [28] to southward drift of the Aldan Shield along the Zhuya strike-slip fault during the late Riphean, the oroclinal form may simply have been the last product of long-term, highly oblique (NE-SW) closure, rather than orthogonal closure of the Aldan Shield against the Akitkan Fold Belt. If so, then the supporting western edge of the Aldan Shield probably extends beneath the Patom metasedimentary cover to at least as far west as the centre of curvature. Local transpression of this magnitude necessitates an identifiable source to the northeast for the oroclinally translated segment. As shown in Fig. 13, there is a geophysically defined basin 5 km in depth now occupied by younger platform sediments lying immediately northeast of the Patom Highlands. This was undoubtedly the original location of the eastern half of the Patom Group prior to final closure of the Akitkan Foldbelt.

CONCLUSIONS

Four distinct stages of ore genesis can be identified in the history of the Sukhoi Log gold deposit:

1. Synsedimentary, syndiagenetic mineralization of marine carbonaceous sediments by density-stratified metalliferous brines, sourced by very large volumes of Au-bearing, deep crustal hydrothermal fluids, and by

PGM-bearing lithospheric mantle-sourced fluids, through rift basin extensional faults; a "mineralizing Yangtze" in the words of Fyfe [54, 55].

2. Disseminated pyrite-gold mineralization (Pyrite I then Pyrite II), developed during penetrative ductile, synmetamorphic deformation and devolatilization, with pervasive fluid transport of gold, PGM, and many other metals from depth in the fold limbs into the anticlinal hinge region. Higher gold grades accumulated in tectonically thickened zones of black shale units (ore pillars) along the anticlinal hinge.

3. Post metamorphic nonpenetrative small-scale flexural folding (F_2) with local segregations at hinge zones of small quartz-gold veins. Elsewhere non-pervasive, small, irregular quartz-pyrite-gold-carbonate veinlets formed in clusters (stringers) and scattered pyrite porphyroblasts with quartz pressure rims (Pyrite II). Finally, a late minor phase of low-gold, coarsely porphyroblastic pyrite developed with little or no quartz, or deformation features (Pyrite III).

4. A widespread development of late stage, large and lengthy, low-grade mesothermal quartz-gold veins, transgressive through the main orebody but probably sourced from it.

Sukhoi Log thus qualifies as a syngenetic-metamorphic Au-PGM deposit and may possibly be an end member of a black shale hosted spectrum that includes sedimentary derived Zn-Pb sedex deposits, mixed sedimentary and crustal sourced Zn-Pb-Ba±Au deposits, and crustal and mantle sourced Au-PGM deposits, all of which occur within the Olokit-Patom terrane.

During the past several years, similar black shale-hosted PGM have been discovered at an increasing number of gold mines and deposits worldwide, which suggests that this mode of mineralization may have occurred as an occasional precursor stage in the development of many orogenic lode-gold deposits. Thus, some presently dormant or extinct black shale-hosted goldfields may yet become large, low-grade economic resources with combined Au-PGM values, which separately would otherwise be subeconomic.

Acknowledgements. The authors wish to acknowledge the insight, skill and dedication of those geologists and workers who discovered and quantified the Sukhoi Log deposit under Siberian conditions of extreme difficulty and discomfort. The members of the geotechnical group were awarded the prestigious Lenin Prize in 1980, and included Vladimir Afanasievich Buryak (leader), Vladimir Feofanovich Dubinin, Vladimir Andreyevich Lisiy, Nikolai Pavlovich Popov, Nikolai Stepanovich Romanchenko and Viktor Efimovich Ryabenko. Bryce Wood also acknowledges the very considerable support of the late Nicolai Popov in obtaining clearance and providing access to technical documents at a time when the deposit was classed as a State Secret and all information was restricted. Also acknowledged are useful discussions and observations with V.V. Distler and colleagues at the Institute of the Geology of Ore Deposits, Petrography, Mineralogy and Geochemistry, Moscow, and with G.L. Mitrofanov and colleagues of the East Siberian Research Institute of Geology, Geophysics and Mineral Resources, Irkutsk. An earlier limited version of this account was presented in 1995 by B.L.Wood on behalf of Star Mining Corporation, Sydney, at a symposium entitled Investment Opportunities in Russia, jointly organized by Moscow State Mining University and the Australian Institute of Mining and Metallurgy. More recent political changes in Russia have resulted in this investment opportunity remaining open.

REFERENCES

1. Buryak, V.A., The process of regional metamorphism influencing development of gold-sulfide mineralization in the central part of the Lena Goldfield. Collected papers "Physical-chemical conditions of magmatism and metasomatism". Third All-Union petrographic symposium, *Science*, 1964.

2. Buryak, V.A., Genesis of sulfide mineralization of Lena gold-bearing region, *Geologiya i Geofizika*, 1, 113–118, 1967.

3. Kazakevich, Yu.P., *Lena gold-bearing region. Vol. 1. Stratigraphy, tectonics, magmatism and occurrences of hard rock gold* [in Russian], 164 pp., Nedra, Moscow, 1971.

4. Neymark, L.A., E.Yu. Rytsk, and O.A. Levchenko, An early Proterozoic-upper Archaean age for the Olokit complex (N. Pre-Baikalia) using U-Pb geochronology, in *Precambrian Geology and Geochronology of the Siberian craton and margins*, 206–222, Nauka, 1990.

5. Rundqvist, D.V., and C. Gillen, *Precambrian ore deposits of the East European and Siberian cratons*, 444 pp., Elsevier, 1997.

6. Salop, L.J., *Geological evolution of the Earth during the pre-Cambrian*, 439 pp., Springer-Verlag, Berlin, 1983.

7. Stakheyev, I.S., A.S. Evoilov, and A.F. Li, *Chemical analysis of ores and enclosing rocks from the deposit of Sukhoi Log*, IRGIREDMET, Irkutsk, 1964.

8. Popov, N.P., Some features of geological composition and interrelation between sulfide mineralization and

gold-quartz mineralization of the Sukhoi Log deposit, in *Issues of Geology and Gold Occurrence in the Lena Region. Collected papers*, 199–204, Irkutsk Polytechnic Institute, Irkutsk, 1969.

9. Popov, N.P., and V.A. Lisiy, The promising type of gold deposits of Siberia, *Subsoil Exploration and Protection*, 7, 5–7, 1974.

10. Buryak, V.A., N.P. Popov, D.A. Dorofeyev, et al., Sukhoi Log deposit, in *Gold deposits of USSR. Vol. 3. Geology of gold deposits of eastern and western Siberia*, 173–186, TsNIGRI, Moscow, 1986.

11. Buryak, V.A., The formation of gold mineralization in graphitic rocks, *Izv. AN SSSR. Ser. Geol.*, 2, 94–105, 1987.

12. Larin, A.M., Ye.Yu. Rytsk, and Yu.M. Sokolov, Baikal-Patom fold belt, in D.V. Rundquist and C. Gillen (eds.), *Precambrian ore deposits or the east European and Siberian cratons. Developments in Economic Geology 30*, 317–362, Elsevier, 1997.

13. Shields, J.W., Gold in greywacke in anticlinal crests — GIGIACS — in the Pine Creek geosyncline, in *Proceedings of the Australian Institute of Mining and Metallurgy Annual Conference*, 68–72, Darwin, 1994.

14. Konstantinov, M.M., E.M. Nekrasov, A.A. Sidorov, and S.F. Struzhkov, *Gold Giants of Russia and World*, 272 pp., Nauchnyi Mir, Moscow, 2000.

15. Zairi, N.M., S.D. Sher, V.P. Strizhov, et al., Isotopic composition of sulfur of the gold-bearing sulfide dissemination zone, *Sovetskaya Geologiya*, 1, 90–98, 1977.

16. Poluarshinov, G.P., and M.V. Konstantinov, New types of platinoid mineralization, *Mineral Resources of Russia*, 20–23, 1994.

17. Laverov, N.P., V.V. Distler, G.L. Mitrofanov, et al., PGE mineralization at the Sukhoi Log gold deposit, eastern Siberia, Russia, in *8th International Platinum Symposium, Johannesburg, Symposium Series S18*, 189–191, 1998.

18. Korobeinikov, A.F., G.L. Mitrofanov, V.K. Nemerov, and N.A. Kolpakova, Nontraditional gold-platinum deposits in East Siberia, *Geologiya i Geofizika (Russian Geology and Geophysics)*, **39**, 4, 432–444(435–447), 1998.

19. Pasava, J., Anoxic sediments — an important environment for PGE: An overview, *Ore Geol. Rev.*, **8**, 425–445, 1993.

20. Kucha, H., Platinum group metals in the Zechstein copper deposits, Poland, *Econ. Geol.*, **77**, 1578–1591, 1982.

21. Coveney, R.M., and C. Nansheng, Ni-Mo-PGE-Au rich ores in Chinese black shales and speculations on possible analogues in the United States, *Miner. Dep.*, **26**, 83–88, 1991.

22. Distler, V.V., M.A. Yudovskaya, and V.Y. Prokof'ev, Hydrothermal migration of PGE, in *31st International Geological Congress: Abstracts Sec. 11.3*, 189–191, Rio de Janeiro, Brazil, 2000.

23. Bejanova, M.P., and H.P. Piskorsky, *Classification of hard economic mineral reserves and resources; principles and special features: Seminar on Modern Methods of Mineral Prospecting (Tbilisi, Georgia, 30 Oct.–10 Nov.)*, 21 pp., Tbilisi, 1989.

24. Subbotin, A.G., and V.M. Zaitseva, Gold and platinum group elements in carbonaceous formations of the Ukranian Carpathians, in *31st International Geological Congress: Abstracts Sec. 11.3*, Rio de Janeiro, Brazil, 2000.

25. Rafailovich, M.S., Large gold and platinum deposits associated with black shales in Kazakhstan, in *31st International Geological Congress: Abstracts Sec. 11.3*, Rio de Janeiro, Brazil, 2000.

26. Jedwab, J., D. Badaut, and P. Beaunier, Discovery of a palladium-platinum-gold-mercury bitumen in the Boss Mine, Clark County, Nevada, *Econ. Geol.*, **94**, 1163, 1999.

27. Rosen, O.M., K.C. Condie, L.M. Natapov, and A.D. Nozhkin, Archean and early Proterozoic evolution of the Siberian craton: a preliminary assessment, in K.C. Condie (ed.), *Archean Crustal Evolution. Chap. 10*, 411–450, Elsevier, 1994.

28. Zonenshain, L.P., M.I. Kuzmin, and L.M. Natapov, Geology of the USSR a plate-tectonic synthesis, in B.M. Page (ed.), *Amer. Geophys. Union, Geodynamic Series*, **21**, chap. 3, 17–30, 1990.

29. Stanevich, A.M., and V.K. Nemerov, Sedimentary-volcanogenic formations of Late Precambrian of the Baikal-Patom Upland: their correlation on the basis of microphytological and geochemical data, *Geologiya i Geofizika (Russian Geology and Geophysics)*, **34**, 3, 56–63(52–59), 1993.

30. Faizullin, M.Sh., New data on Baikalian microfossils of the Patom Upland, *Geologiya i Geofizika (Russian Geology and Geophysics)*, **39**, 3, 328–337(338–347), 1998.

31. Khomentovsky, V.V., A.A. Postnikov, and M.Sh. Faizullin, The Baikalian in the type locality, *Geologiya i Geofizika (Russian Geology and Geophysics)*, **39**, 11, 1505–1517(1505–1516), 1998.

32. Konnikov, E.G., A.S. Gibsher, A.E. Izokh, E.V. Sklyarov, and E.V. Khain, Late-Proterozoic evolution

of the northern segment of the Paleoasian Ocean: new radiological, geological, and geochemical data, *Geologiya i Geofizika (Russian Geology and Geophysics)*, **35**, 7–8, 152–168(131–145), 1994.

33. Bulgatov, A.N., Riphean sedimentary-volcanogenic complexes of the Mid-Vitim region (Transbaikalia): geodynamic and facies conditions of their formation, *Geologiya i Geofizika (Russian Geology and Geophysics)*, **36**, 7, 34–41(31–38), 1995.

34. Khomentovsky, V.V., The event nature of the Neoproterozoic Stratigraphic Scale for Siberia and China, *Geologiya i Geofizika (Russian Geology and Geophysics)*, **37**, 8, 43–56(35–47), 1996.

35. Nemerov, V.K., and A.M. Stanevich, Evolution of the Riphean-Vendian biolithogenesis settings in the Baikal mountainous area, *Geologiya i Geofizika (Russian Geology and Geophysics)*, **42**, 3, 456–470(444–458), 2001.

36. Coleman, R.G., *Ophiolites — ancient oceanic lithosphere?*, Berlin-Heidelberg-New York, 1977.

37. Kepezhinkas, K,B., L.A. Dagis, L.S. Zorkina. and N.A. Prusevich, The chemistry of the metavolcanites in ophiolitic complexes as an indicator of various paleotectonic environments, *Geologiya i Geofizika (Soviet Geology and Geophysics)*, **25**, 2, 11–24(9–20), 1984.

38. Neymark, L.A., Ore Pb isotopes and the origin of deposits, in *Isotope Geochemistry of Ore-forming Processes*, 99–116, Nauka, Moscow, 1988.

39. Neymark, L.A., A.M. Larin, and S.Z. Yakovleva, New data on the age of the Akitkan group in the Baikal-Patom foldbelt, from results of U-Pb dating of zircons, *Dokl. AN SSSR*, **320**, 1, 182–186, 1991.

40. Rundqvist, D.V., Geological evolution and metallogeny of the Baikalides, in *Fundamental Problems in Ore Formation and Metallurgy*, 44–65, Nauka, Leningrad, 1990.

41. Hannington, M.D., P.M. Herzig, and S.D. Scott, Auriferous hydrothermal precipitates on the modern seafloor, in R.P. Foster (ed.), *Gold metallogeny and exploration*, 249–275, Blackie, Glasgow, 1991.

42. Thorkelson, D.J., Subduction of converging plates and principles of slab window formation, *Tectonophysics*, **225**, 47–63, 1969.

43. Hilde, T.W.C., Sediment subduction versus accretion around the Pacific. Convergence and subduction, *Tectonophysics*, **99**, 381–397, 1983.

44. Haeussler, P.J., B. Bradley, R. Goldfarb, L.W. Snee, and C.D. Taylor, Link between ridge subduction and gold mineralization in southern Alaska, *Geology*, **23**, 11, 995–998, 1995.

45. Mapani, B.E.S., and C.J.L. Wilson, Evidence for externally derived vein forming and mineralising fluids: an example from the Magdala gold mine, Stawell, Victoria, Australia, *Ore Geol. Rev.*, **13**, 323–343, 1998.

46. Sisson, V.B., and T.L. Pavlis, Geological consequences of plate reorganisation: an example from the Eocene southern Alaska fore-arc, *Geology*, **21**, 913–916, 1993.

47. Pohl, W., Defining metamophogenic mineral deposits — an introduction, *Miner. Petrol.*, **45**, 145–152, 1992.

48. Beveridge, T.J., and R.G.E. Murray, Uptake and retention of metals by cell walls of Bacillus subtilis, *J. Bacterial.*, **127**, 1502–1518, 1976.

49. McCuaig, T.C., and R. Kerrich, *P-T-t*-deformation-fluid characteristics of lode gold deposits: evidence from alteration systematics, *Ore Geol. Res.*, **12**, 381–453, 1998.

50. Guilbert, J.M., and C.F. Park, *The geology of ore deposits*, 630–659, Freeman and Co., New York, 1996.

51. Emsbo, P., R.W. Hutchinson, A.H. Hofstra, J.A. Volk, K.H. Bettles, G.J. Baschuk, and C.A. Johnson, Syngenetic Au on the Carlin Trend; implications for carlin-type deposits, *Geology*, **27**, 1, 59–62, 1999.

52. Emsbo, P., Gold in sedex deposits, *Reviews in Economic Geology*, **13**, 427–437, 2000.

53. Carey, S.W., The oroclinal concept in geotectonics, *Proc. Royal Soc. Tasmania*, Ppr. 89, 255–287, 1955.

54. Fyfe, W.S., Tectonics, fluids and ore deposits: mobilization and remobilization, *Ore Geol. Rev.*, **2**, 21–36, 1987.

55. Fyfe, W.S., Gold transport and deposition: Rules of the game, in E.A. Ladeira (ed.), *Brazil Gold'91*, Rotterdam, Balkema, 1991.

Editorial responsibility: R. Coleman

Received 29 December 2004